

# Dynamo regime transition among Sun-like stars in M 34<sup>★,★★</sup>

## A time evolution model of X-ray activity on the main sequence

P. Gondoin

European Space Agency, ESTEC – Postbus 299, 2200 AG Noordwijk, The Netherlands  
e-mail: pgondoin@rssd.esa.int

Received 15 June 2012 / Accepted 16 August 2012

### ABSTRACT

**Context.** The X-ray emission from late-type stars in open clusters exhibits two kinds of dependences on stellar rotation. While fast rotators have a relatively constant X-ray emission level, slower rotators show a decline of their X-ray emission with decreasing rotation rate. The physical significance of the transition between these two X-ray emission regimes is a matter of debate. During the ~500 Myr period of stellar evolution that separates the Pleiades from the Hyades, late-type stars such as those present in the M 34 open cluster undergo significant changes in their rotation rates. These could affect the dynamo processes in their interiors, possibly altering their surface magnetic fluxes.

**Aims.** The purpose of the present study is to look for the X-ray signatures of such possible modifications, to search for correlations with rotation and stellar parameters, and to propose a parameterization of the X-ray activity evolution on the main sequence. The aim is to provide observational constraints on the time evolution of dynamo processes in the interiors of late-type stars.

**Methods.** The distributions of stellar X-ray luminosities vs. rotation periods and Rossby numbers of a sample of M 34 late-type stars are compared with rotation-activity relationships established in a large sample of cluster members and field stars. A model of X-ray activity evolution is developed by combining an X-ray activity-rotation relationship with a recent model of stellar rotation evolution on the main sequence. The distribution of stellar X-ray luminosities in M 34 is compared with this model.

**Results.** A correlation is observed between the saturated and non-saturated regime of X-ray emission and the C- and I-rotational sequences that have been observed in M 34 from extensive rotational periods surveys. M 34 sample stars show a steep transition in X-ray to bolometric luminosity ratio between the C-sequence and gap stars that emit close to the  $10^{-3}$  saturation level, and the I-sequence stars, whose  $L_X/L_{\text{bol}}$  ratio is significantly lower for similar values of the Rossby number. A comparison between X-ray emission vs. mass distribution in M 34 and the X-ray luminosity evolution model suggests that the transition between the saturated and non-saturated regime of X-ray emission occurs in M 34 cluster members depending on their convective turnover time and period of rotation.

**Conclusions.** I argue that the drop of ( $L_X/L_{\text{bol}}$ ) by one order of magnitude observed in M 34 around a Rossby number of 0.3 is indicative of a change in dynamo efficiency. I conclude that the transition from the saturated to the non-saturated regime of X-ray emission among main-sequence stars is the result of a dynamo regime transition, possibly between a turbulent dynamo and an interface-type dynamo.

**Key words.** open clusters and associations: individual: M 34 – stars: activity – stars: atmospheres – stars: late-type – stars: magnetic field – stars: rotation

## 1. Introduction

The present paper reports on the results of a study of X-ray coronal emission as a function of stellar rotation in the M 34 open cluster. M 34 (NGC 1039;  $\alpha = 02^{\text{h}}42^{\text{m}}06^{\text{s}}$ ,  $\delta = 42^{\circ}46'$ ;  $l = 143.7^{\circ}$ ,  $b = -15.6^{\circ}$ ) is located at a distance of about 470 pc (Jones & Prosser 1996). Its metallicity is close to solar ( $[\text{Fe}/\text{H}] = 0.07 \pm 0.04$ ; Schuler et al. 2003). Estimates of its age derived from fitting stellar evolution isochrones to the cluster color magnitude diagrams range from 177 Myr (Meynet et al. 1993) to 251 Myr (Ianna & Schlemmer 1993). Ages of  $198 \pm 9$  Myr (James et al. 2010) and 240 Myr (Meibom et al. 2011) have been derived recently using the gyrochronology technique (Barnes 2007).

\* Based on observations obtained with *XMM-Newton*, an ESA science mission with instruments and contributions directly funded by ESA Member States and NASA.

\*\* Tables 1 and 2 are available in electronic form at <http://www.aanda.org>

The X-ray emission from late-type stars in open clusters exhibits two kinds of dependences on stellar rotation (Patten & Simon 1996; Randich 2000; Feigelson et al. 2003). Fast rotators show a relatively constant X-ray emission at the ( $L_X/L_{\text{bol}}$ )  $\approx 10^{-3}$  saturation level derived by Pizzolato et al. (2003). Slower rotators show a decline of their X-ray emission with decreasing rotation rate.

The physical significance of the transition between these two X-ray emission regimes is a matter of debate (e.g., Jardine & Unruh 1999). Correlations between rotation sequences and X-ray emission regimes were searched by Barnes (2003b). More recently, the association of the two X-ray emission regimes with different dynamos was explored by Wright et al. (2011).

M 34 is evolving at an age intermediate between that of the Pleiades (~125 Myr, e.g., Stauffer et al. 1998) and that of the Hyades (~625 Myr, e.g., Perryman et al. 1998). While stars in the Pleiades rotate at rates between 0.2 and 10 days (Hartman et al. 2010), stars in the Hyades are in general much slower rotators (e.g., Delorme et al. 2011). During the ~500 Myr time

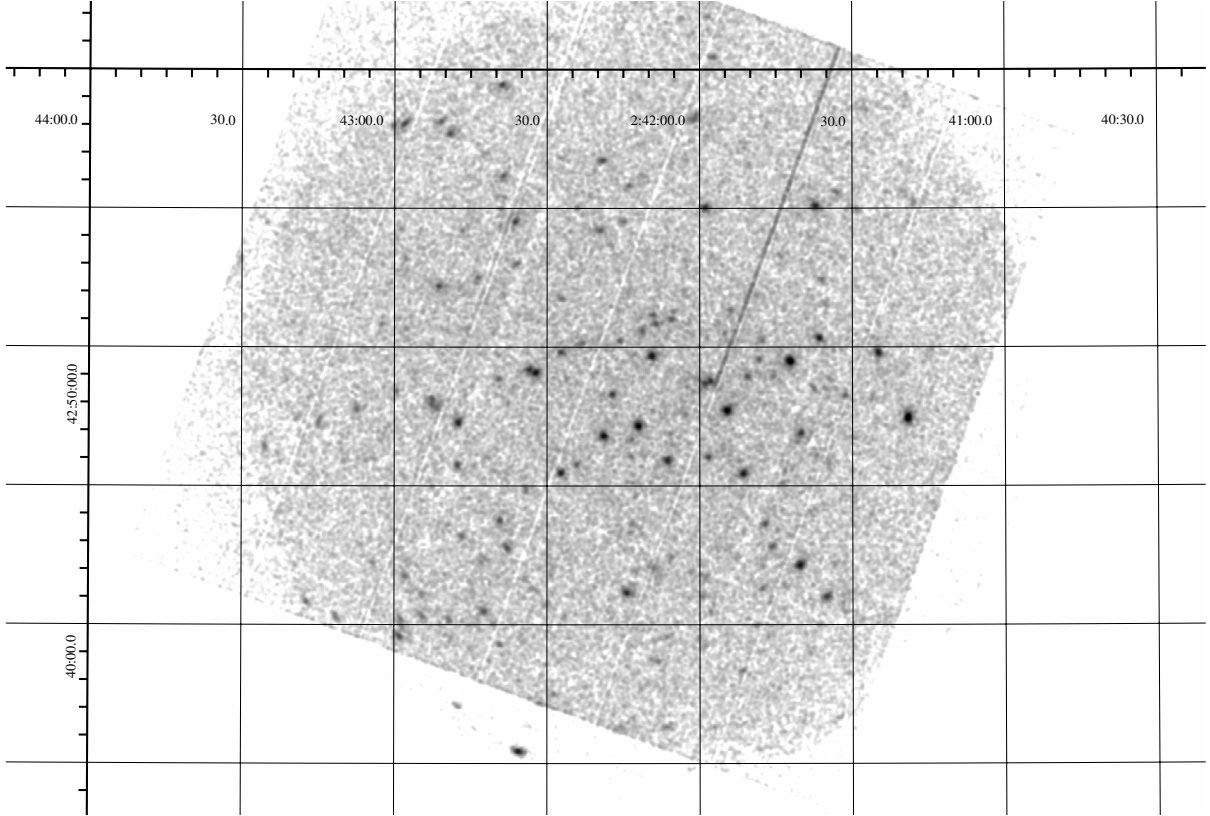


**Fig. 1.** Combined MOS1, MOS2, and PN image of NGC 1039 in the 0.5 to 4.5 keV band.

interval that separates these two clusters, late-type stars such as those present in M 34 thus undergo significant changes in their surface rotation rate. These changes are the visible signature of modifications of their internal rotation profiles. These, in turn, could affect the dynamo processes that operate in their interiors, possibly altering the level of magnetic activity in their outer atmospheres. The purpose of the present study is to look for the X-ray signatures of such possible modifications, to search for correlations with rotation and stellar parameters, and to propose a parameterization of the X-ray activity evolution on the main sequence. The aim is to provide observational constraints on the time evolution of dynamo processes in the interiors of late-type stars.

A previous X-ray observation of M 34 with the ROSAT High Resolution Imager has been reported by Simon (2000), who found some indication that solar-type stars in this cluster and in the similarly aged NGC 3532 and NGC 6475 lack the extreme rotation and activity levels shown by those in the much younger Pleiades and  $\alpha$  Persei clusters. The present study benefits from high throughput observations of M 34 with the *XMM-Newton* satellite observatory and from measurement surveys of stellar rotation periods in M 34 that have been recently published by Irwin et al. (2006, hereafter I06), James et al. (2010, hereafter J10), and Meibom et al. (2011, hereafter M11).

The observational data and the compilation of the sample stars are described in Sect. 2. The data analysis is reported in Sect. 3. A model of X-ray activity evolution is presented in Sect. 4. The stellar X-ray emission in M 34 is compared with the model in Sect. 5. The study results are discussed in Sect. 6 and summarized in Sect. 7.

## 2. Compilation of the sample

### 2.1. Observational data

M 34 was observed by the *XMM-Newton* space observatory (Jansen et al. 2001) on 12 February 2003. The observations were conducted with the EPIC pn CCD camera (Strüder et al. 2001) and the two EPIC MOS cameras (Turner et al. 2001) located at the prime focus of the three grazing incidence telescopes (Gondoin et al. 2000). The EPIC pn and MOS cameras exposure times were 42 ks and 39 ks, respectively (see Fig. 1). A “thick” aluminum filter was used in front of the cameras to reject visible light from the stars. Detection was made of 189 X-ray sources that are listed in the *XMM-Newton* Serendipitous Source Catalog (Watson et al. 2009).

The X-ray data were complemented by recent measurement results of stellar rotation periods. The *XMM-Newton* X-ray source list was first correlated with the list of 83 kinematic and photometric late-type M 34 cluster members with known rotation periods established by M 11. In order to estimate the optimal radius of cross correlation, I used the approach outlined by Jeffries et al. (1997). The cumulative distribution of the number of detected sources was generated as a function of the cross-correlation radius (see Fig. 2). It was fitted by the following function:

$$\Phi(r) = A \times \left(1 - \exp\left(-\frac{r^2}{2\sigma^2}\right)\right) + (N - A) \times \left(1 - \exp(-\pi B r^2)\right) \quad (1)$$

where  $N$ ,  $A$ ,  $\sigma$ , and  $B$  stand for the total number of cross-correlated X-ray sources ( $N = 189$ ), the number of true correlations, the uncertainty on the X-ray source positions, and the surface density of optical sources, respectively. The first term

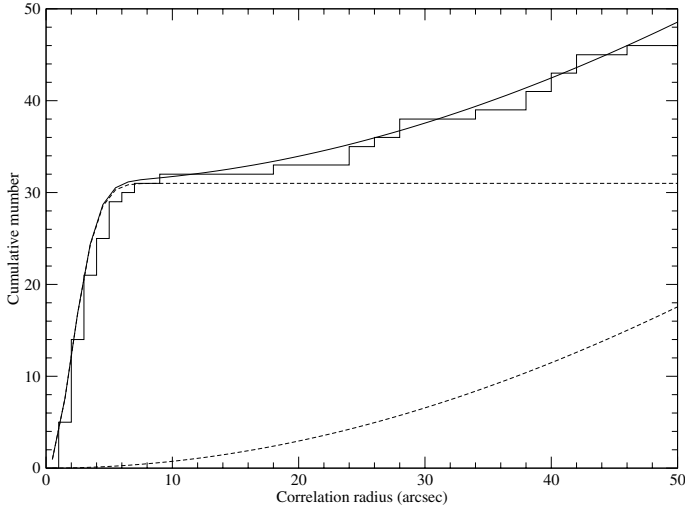


**Fig. 2.** Cumulative numbers of correlations between the X-ray detections and the M 34 time-series photometric survey of M 11. The dotted curves correspond to the best fitting expressions for the real and spurious correlations. The continuous curve yields the sum of these terms.

in the above expression describes the cumulative distribution of true correlations, whereas the second term yields the cumulative number of spurious correlations. The values  $A = 31$ ,  $\sigma = 2.0$  arcsec, and  $B = 1.5 \times 10^{-5}$  arcsec $^{-2}$  were obtained from the best fit to the cumulative distribution (see Fig. 2). The optimal correlation radius, i.e., the radius that includes the bulk of the true correlations while simultaneously limiting contamination by spurious correlations, is found to be about 7 arcsec. For this radius, 31 correlations have been found, and less than one is expected to be spurious, indicating that all sources of the M 11 list that are located in the EPIC field of view have been detected as X-ray emitters.

The *XMM-Newton* X-ray source list was then correlated with the results of a time series photometric survey of M 34 in the V- and i-bands reported by I06. These authors measured the rotation periods of 105 cluster members selected from a  $V$  vs.  $V - I$  color-magnitude diagram covering a magnitude range  $14 < V < 24$ . Among these sources, 34 are located in the EPIC field of view. The optimal radius of cross correlation was determined as described previously. Best-fit parameters of the cumulative distribution (see Eq. (1)) are  $A = 21$ ,  $\sigma = 1.9$  arcsec, and  $B = 1.45 \times 10^{-5}$  arcsec $^{-2}$ . The optimal correlation radius is found to be about 5 arcsec. For this radius, 20 correlations are found and less than one is expected to be spurious. Of these 20 correlations, eight are new since 12 sources were already detected in the correlation between the M 34 X-ray source list and the M 11 list.

Finally, the *XMM-Newton* source list was correlated with the list of 55 solar-type stars in M 34, whose rotation periods were derived from differential photometry by J10. Among these sources, 15 were located in the EPIC field of view observed in February 2003 with *XMM-Newton*. The optimal radius of cross correlation was determined as described previously. Values  $A = 7$ ,  $\sigma = 1.0$  arcsec, and  $B = 1 \times 10^{-5}$  arcsec $^{-2}$  were obtained for the best-fit parameters of the cumulative distribution. The optimal correlation radius is found to be 3 arcsec for which seven correlations have been found that are expected to be true. Only two of these correlations are new.

In total, 41 stellar members of the M 34 open cluster have been found that have known rotational periods and for which

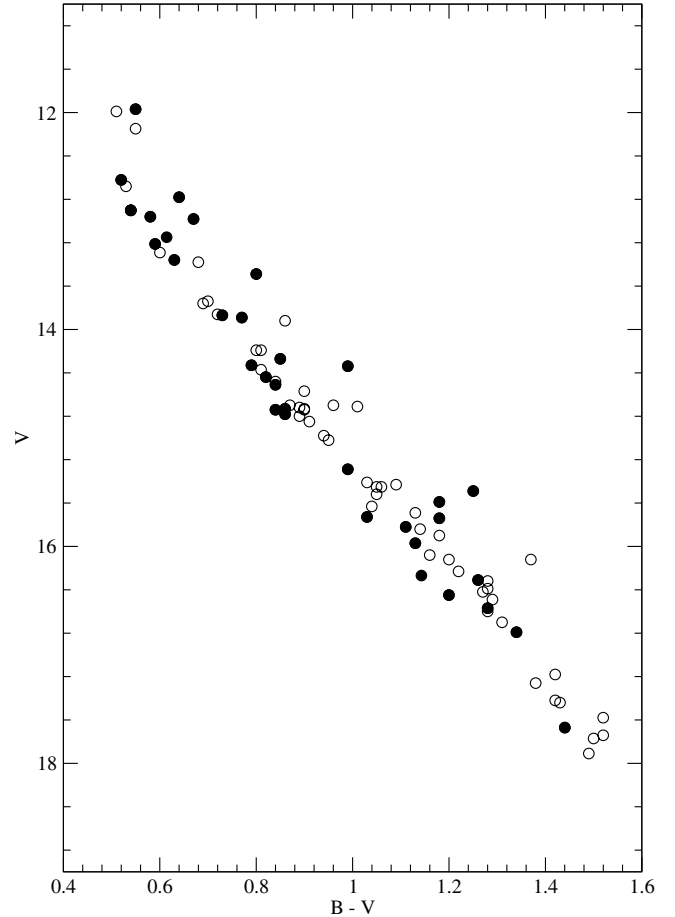


**Fig. 3.**  $V$  vs.  $B - V$  color magnitude diagram of M 34 in the range  $12 < V < 18$ . Open circles represent M 34 cluster members that M 11 found to be either photometric, proper-motions (Jones & Prosser 1996), or radial velocity cluster members. Filled circles represent stellar members that have been detected as X-ray sources in the EPIC field of view and whose rotational periods have been photometrically determined by M 11 and J10.

X-ray emission has been detected. Table 1 lists the M 11, I06, J10, and *XMM-Newton* catalog identifiers of these sample stars. It provides their X-ray count rates, rotational periods,  $V_0$  magnitudes corrected for extinction, and  $(B - V)_0$  color indices corrected for reddening by M 11 and J10. The position of these stars in a  $V$  vs.  $B - V$  color magnitude diagram is given in Fig. 3. Table 1 also provides the  $V - I$  color index of the I06 sample stars.

## 2.2. Derivation of stellar parameters and X-ray luminosities

I used the effective temperature and bolometric correction vs.  $B - V$  color index of Flower (1996) to derive the effective temperatures and bolometric luminosities of the J10 and M 11 sample stars. A true M 34 distance modulus of 8.38 (Jones & Prosser 1996) was assumed. Since the I06 sample stars have unknown  $V_0$  and  $(B - V)_0$ , I used the  $T_{\text{eff}}$  vs.  $V - I$  relation established by Casagrande et al. (2010) with a reddening correction  $E_{V-I} = 1.25 \times E_{B-V}$  and  $E_{B-V} = 0.07$  (Canterna et al. 1979) to determine their effective temperature. The bolometric luminosities of these stars were then calculated from the stellar radii provided in I06.

X-ray fluxes were derived from the source count rates using energy conversion factors (ECF). In the *XMM-Newton* catalog,

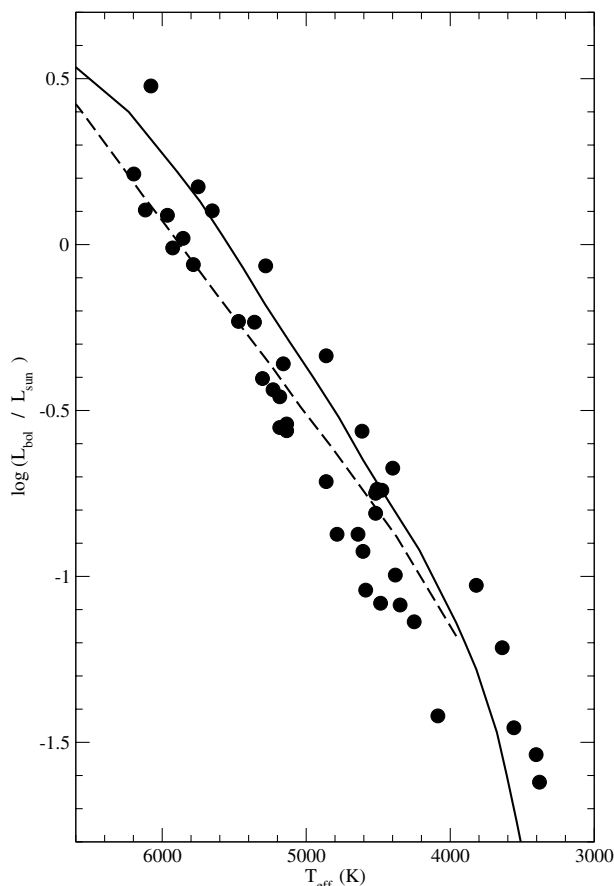


**Fig. 4.** HR diagram positions of the sample stars with known X-ray luminosity and rotation periods compared with the 200 Myr NextGen isochrones of Baraffe et al. (1998) for solar metallicity with mixing length parameters  $L_{\text{mix}} = H_p$  (solid line) and  $L_{\text{mix}} = 1.9H_p$  (dashed line).

these factors are calculated from a broadband source spectrum that is assumed to be characterized by a power law with a photon index  $\Gamma = 1.7$  and an X-ray absorption  $N_{\text{H}} = 3 \times 10^{20} \text{ cm}^{-2}$  (Watson et al. 2009). This model provides a reasonable representation of the emission of the bulk of the sources in the 2XMMi-DR3 catalog, but does not provide a priori a suitable flux conversion for stellar coronae. To estimate the X-ray luminosities of the M 34 sample stars, I use instead energy conversion factors calculated using the Portable, Interactive, Multi-Mission Simulator (PIMMS; Mukai 1993) in the 0.5–4.5 keV range for optically thin plasmas with temperatures comparable to those found in the spectral fitting of active stellar coronae (see Gondoin 2006). The absorbing hydrogen column density towards M 34 is estimated from the reddening correction  $E_{B-V} = 0.07$  (Canterna et al. 1979) to about  $3.4 \times 10^{20} \text{ cm}^{-2}$ . For absorbing hydrogen column densities lower than  $10^{21} \text{ cm}^{-2}$ , the energy conversion factor of the EPIC pn camera equipped with a thick filter in the 0.5–4.5 keV band is flat and well approximated by  $\text{ECF} = 3.7 \times 10^{11} \text{ counts erg}^{-1} \text{ cm}^2$  for plasma temperatures in the range  $(4\text{--}25) \times 10^6 \text{ K}$  (see Gondoin 2006; Fig. 4). The X-ray fluxes were then converted into stellar X-ray luminosities assuming a distance of 470 pc (Jones & Prosser 1996).

The X-ray luminosities, bolometric luminosities, effective temperatures, masses, radii, and rotation periods of M 34 sample stars are given in Table 2.

### 3. Analysis

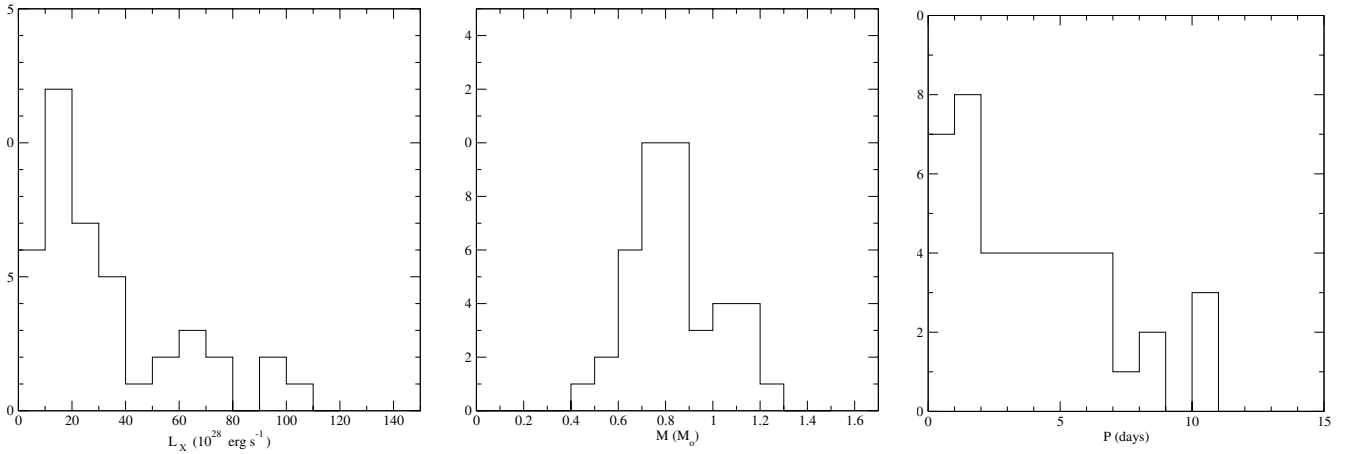
#### 3.1. Sample properties

Figure 4 compares the HR diagram positions of the sample stars having known X-ray luminosities and rotation periods with the 200 Myr isochrones of Baraffe et al. (1998) evolution models for solar metallicity with mixing length parameters  $L_{\text{mix}} = H_p$  (solid line) and  $L_{\text{mix}} = 1.9H_p$  (dashed line). A good agreement is obtained when using a true M 34 distance modulus of 8.38 (Jones & Prosser 1996). Assuming that the upper envelope of the M 34 color magnitude diagram is dominated by photometric binaries, a fit to the lower envelope would give a larger distance. The brightest M 34 source (with a known X-ray luminosity and rotational period) has a magnitude  $V = 11.97$  and a color index  $B - V = 0.55$  corresponding to an effective temperature of approximately 6000 K (Flower 1996) and a F9 spectral type on the main sequence. The faintest X-ray source with a known rotational period has a magnitude  $V = 18.81$  and a color index  $V - I = 2.35$  corresponding to a mass  $M \approx 0.49 M_{\odot}$  and a M3 spectral type.

The distributions of the sample stars as a function of X-ray luminosity, mass, and rotation period are described in the histograms of Fig. 5. The X-ray luminosity histogram (Fig. 5 left) rolls off at luminosities lower than  $L_X \approx 10^{29} \text{ erg s}^{-1}$ , which provides a sensitivity limit estimate of the EPIC observation conducted in February 2003.

The mass histogram (see Fig. 5 middle) of the sample stars covers a range included between  $0.4 M_{\odot}$  and  $1.3 M_{\odot}$ . The number of detected stars per mass interval reaches a maximum around  $0.8 M_{\odot}$ , while it should keep increasing towards lower masses. The I06 sample includes rotation period measurements on stars below  $0.4 M_{\odot}$ . Some of them were present in the field of view of the *XMM-Newton* EPIC camera, but were not detected in X-rays most likely because of their low X-ray luminosities. Indeed, the X-ray luminosities of the sample stars tend to decrease with decreasing stellar masses (see Fig. 8 left). The trend indicates that stars less massive than about  $0.5 M_{\odot}$  are likely to fall below the X-ray detection threshold. Only one such star, XMM J024234.8+423926 ( $M = 0.49 M_{\odot}$ ), has been detected with an X-ray luminosity of  $7.8 \pm 2.9 \times 10^{28} \text{ erg s}^{-1}$ .

The present sample is mainly issued from the M 11 sample. Its distribution in rotation periods (see Fig. 5 right) extends from 0.49 days to 11 days as does the M 34 stellar sample studied by M 11. Since the photometric measurement protocol of M 11 was sensitive to a range of periods extending from a 0.08 day pseudo-Nyquist limit up to 23 days, these authors suggested that 11.5 days is a physical upper limit of the rotation period distribution among F, G, and K dwarfs in M 34. The existence of such a limit is consistent with the results presented by I06, who noticed a lack of slow rotators ( $P \geq 5$  days) at low masses ( $M < 0.4 M_{\odot}$ ). However, the observing run of these authors only extended over ten nights. With a 17-night observing run, J10 reported nine stars with a period larger than 11.5 days. The X-ray luminosity vs. rotation period plot (see Fig. 7 left) of the sample stars shows that X-ray luminosity tends to decrease with increasing rotation periods. The trend suggests that stars rotating slower than about ten days likely fall below the X-ray detection threshold of the *XMM-Newton* observation in February 2003. Only two such slow rotators, XMM J024220.4+424905 ( $P = 10.99 \text{ d}$ ) and XMM J024243.6+425230 ( $P = 10.75 \text{ d}$ ), have been detected with X-ray luminosities of  $4.5 \pm 1.6 \times 10^{28} \text{ erg s}^{-1}$  and  $19.5 \pm 3.5 \times 10^{28} \text{ erg s}^{-1}$ , respectively.



**Fig. 5.** X-ray luminosity (*left*), mass (*middle*), and rotation period (*right*) histograms of the sample stars.

### 3.2. X-ray luminosities of Sun-like stars in M 34

Among the 41 sample stars listed in Table 2, 21 have masses included between  $0.8 M_{\odot}$  and  $1.2 M_{\odot}$ . The X-ray luminosities of these Sun-like stars are included between  $2 \times 10^{28} \text{ erg s}^{-1}$  and  $10^{30} \text{ erg s}^{-1}$ . Large spreads in X-ray luminosity of more than one order of magnitude among stars with the same age and similar masses have been observed in many open clusters including the Pleiades, the Hyades (e.g., Stern et al. 1995; Micela et al. 1996), and NGC 752 (Giardino et al. 2008). A large spread in X-ray luminosity has also been noted among field stars. In particular, G-type field stars have X-ray luminosities distributed over three orders of magnitude between  $3 \times 10^{26} \text{ erg s}^{-1}$  and  $3 \times 10^{29} \text{ erg s}^{-1}$  with a median value of  $2 \times 10^{27} \text{ erg s}^{-1}$  (Schmitt et al. 1995; Schmitt 1997).

Figure 6 compares the X-ray luminosities of Sun-like stars in M 34 with corresponding distributions in  $\alpha$  Per (Randich et al. 1996), in the Pleiades (Micela et al. 1999), in the Hyades (Stern et al. 1995), and among nearby field stars (Schmitt 1997), including the Sun (Peres 2001). The data points are median values of the distributions reported by Micela (2002) and refer to stars within the same mass range ( $0.8 M_{\odot} - 1.2 M_{\odot}$ ). The size of the vertical bars are determined by the 25% and 75% quartiles of the distributions. These quartiles for M 34 stars with  $0.8 \leq M/M_{\odot} \leq 1.2$  correspond to X-ray luminosities of  $1.6 \times 10^{29} \text{ erg s}^{-1}$  and  $6.4 \times 10^{29} \text{ erg s}^{-1}$ , respectively. Figure 6 shows that the median luminosity of the M 34 Sun-like stars detected in X-rays ( $\approx 3 \times 10^{29} \text{ erg s}^{-1}$ ) is two orders of magnitude higher than that of similar field stars. It is slightly higher than the corresponding median luminosity of Sun-like stars in the Hyades and comparable with the X-ray luminosity distribution of Sun-like stars in the Pleiades. Since M 34 is evolving at an age intermediate between that of the Pleiades, the X-ray luminosity distribution of M 34 Sun-like stars thus looks consistent with the decay of average X-ray luminosities with age that has been documented in many studies of open clusters (e.g., Randich 1997; Jeffries 1999; Micela 2001).

### 3.3. X-ray emission vs. rotation period in M 34

The commonly accepted explanation for the decay of average X-ray luminosities with age is that the magnetic activity in late-type stars is regulated principally by rotation, which decays with stellar age due to rotational braking by stellar winds (Schatzman 1962; Kawaler 1988). The correlation between stellar rotation

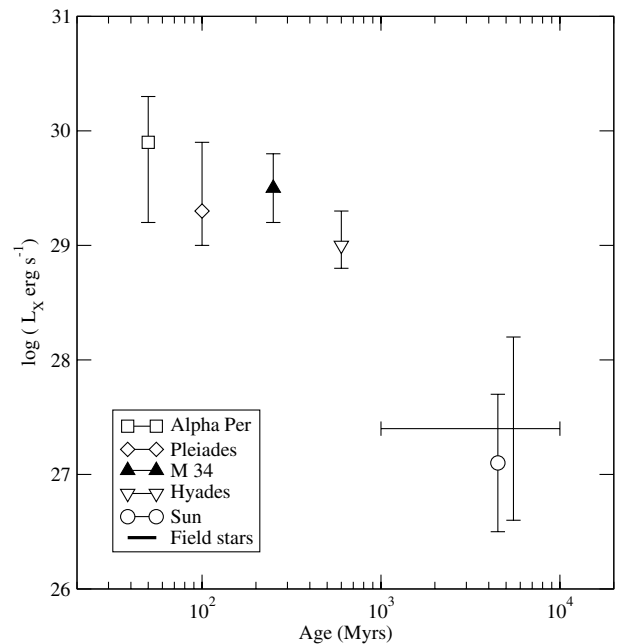


**Fig. 6.** X-ray median luminosity of M 34 sample stars with mass between  $0.8 M_{\odot}$  and  $1.2 M_{\odot}$  compared with median luminosities of stars with the same mass in the  $\alpha$  Per, Pleiades, Hyades, and field stars from Micela (2002). The sizes of the vertical error bars indicate the 25% and 75% quartiles of the distributions.

and X-ray luminosity was first quantified by Pallavicini et al. (1981), who found a relationship  $L_X (\text{erg s}^{-1}) \approx 10^{27} (\nu \sin i [\text{km s}^{-1}])^2$  for an ensemble of F7- to M5-type stars of all luminosity classes. For very fast rotators, Micela et al. (1985) found afterwards that the relationship breaks down at high rotation rates, with X-ray luminosity reaching a saturation level of  $L_X/L_{\text{bol}} \approx 10^{-3}$ .

The correlation between X-ray emission and rotation was analyzed in detail by Pizzolato et al. (2003) as a function of stellar mass. Their sample of main-sequence stars consisted of 110 field stars and 149 members of open clusters, which include the Pleiades, the Hyades,  $\alpha$  Persei, IC 2602, and IC 2391. Figure 7 compares the results of their analysis with the distribution of X-ray luminosity vs. rotation period in M 34. The dashed lines represent the lower and upper limits of the  $L_X$  vs.  $P_{\text{rot}}$  correlation functions quantified by Pizzolato et al. (2003);

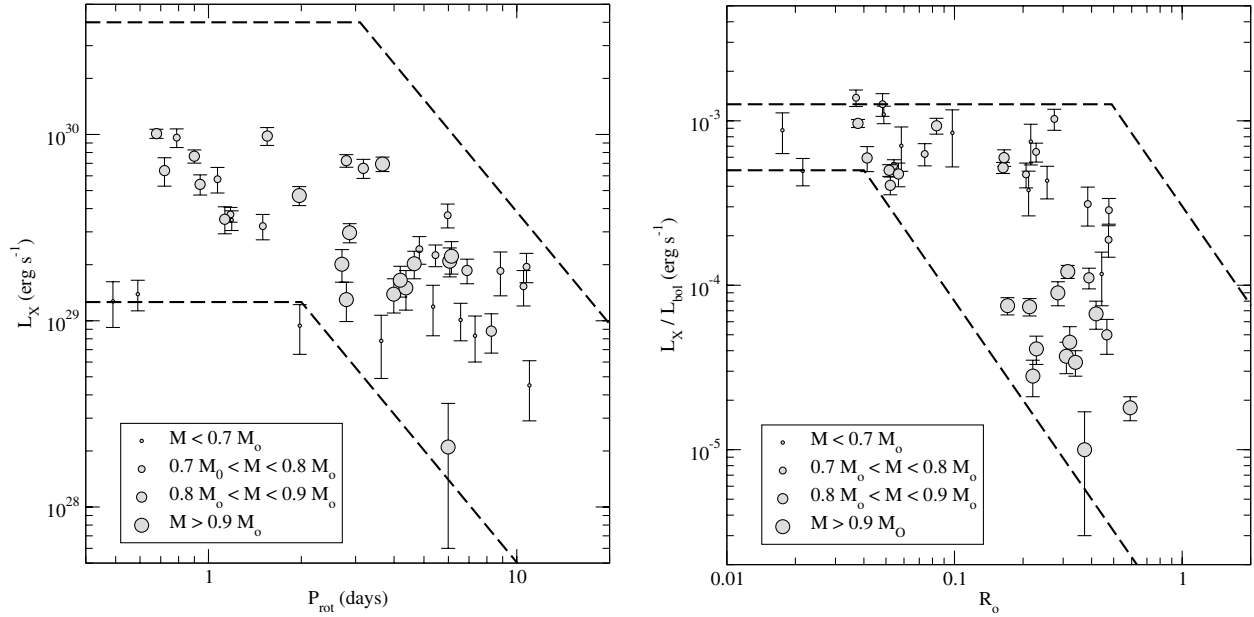


**Fig. 7.** *Left:* X-ray luminosities of the M 34 sample stars vs. rotation periods. *Right:* X-ray to bolometric luminosity ratios vs. Rossby numbers. The mass of each star is indicated by the size of the associated circle. The dashed lines represent the lower and upper limits of the correlation results  $L_X$  vs.  $P_{\text{rot}}$  and  $L_X/L_{\text{bol}}$  vs.  $R_o$  established by Pizzolato et al. (2003) for masses in the range  $0.63\text{--}0.78 M_{\odot}$  (lower curve) and  $1.03\text{--}1.10 M_{\odot}$  (upper curve), respectively.

see Table 3) for stars with  $0.63 < M/M_{\odot} < 0.78$  (lower curve) and  $1.03 < M/M_{\odot} < 1.10$  (upper curve), respectively. The X-ray luminosities of the M 34 sample stars are included between these two envelopes. In particular, Fig. 7 shows that M 34 stars with a rotation period shorter than about three days reach the so-called saturation regime observed on rapidly rotating field stars and members of open clusters.

Seven of the M 34 sample stars have masses in the range  $0.9 < M/M_{\odot} < 1.10$ . Their rotation periods are included between 2.80 and 6.14 days while their X-ray luminosities are in the range  $(13\text{--}30) \times 10^{28} \text{ erg s}^{-1}$ . These M 34 sample stars do not show a tight correlation between their X-ray luminosities and rotation periods, although their average product  $\langle L_X \times P^2 \rangle$  is comparable with the solar value.

### 3.4. X-ray emission vs. Rossby number in M34

Durney & Latour (1978) argued that the activity level of main-sequence stars should rather be a function of the rotation period,  $P_{\text{rot}}$ , divided by a convective turnover time scale  $\tau_c$ . The Rossby number ( $Ro = P_{\text{rot}}/\tau_c$ ) is an important indicator in hydromagnetic dynamo theory that measures the extent to which rotation can induce both helicity and differential rotation, which are considered essential for a solar-type dynamo. The dependence of the X-ray luminosity relative to the bolometric luminosity on the Rossby number was confirmed for F5 through M5 main-sequence stars using both clusters and field stars (e.g., Patten & Simon 1996; Randich et al. 2000).

While the rotation period can be directly measured,  $\tau_c$  is sometimes derived from the mixing-length theory (e.g., Kim & Demarque 1996) and usually empirically determined (Noyes et al. 1984; Stepien 1994; Gilliland 1985; Pizzolato et al. 2001). The determination provided by Noyes et al. (1984) is the most used in the literature, but is based on only a few points redder than  $B - V = 1.0$ . Pizzolato et al. (2003) provided improved

values using a sample with a greater coverage of low-mass stars. Based on these consolidated values, Wright et al. (2011) suggested that the stellar mass is the relevant physical parameter that determines the convective turnover time and derived the following relationship:

$$\log(\tau_{c,w}) = 1.16 - 1.49 \times \log\left(\frac{M}{M_{\odot}}\right) - 0.54 \times \log^2\left(\frac{M}{M_{\odot}}\right). \quad (2)$$

This relationship is valid over the range  $0.09 M_{\odot} < M < 1.36 M_{\odot}$ . It is scaled such that values of  $\tau_{c,w}$  for solar-mass stars match those of Noyes et al. (1984) for the Sun. Equation (2) was used to estimate the Rossby numbers of the sample stars (see Table 2).

Figure 7 (right) displays the X-ray to bolometric luminosity ratio  $L_X/L_{\text{bol}}$  of the M 34 sample stars as a function of the Rossby number  $Ro$ . These data are compared with the lower and upper limits of the  $L_X/L_{\text{bol}}$  vs.  $Ro$  correlation functions quantified by Pizzolato et al. (2003; see their Table 3) for field stars and members of open clusters with  $0.63 < M/M_{\odot} < 0.78$  (lower dashed curve) and  $1.03 < M/M_{\odot} < 1.10$  (upper dashed curve), respectively.

The dispersion of the data points in the  $L_X/L_{\text{bol}}$  vs.  $Ro$  graph (Fig. 7, right) is lower than in the the  $L_X$  vs.  $P_{\text{rot}}$  plot (Fig. 7, left). For Rossby numbers smaller than  $\sim 0.1$ , the X-ray to bolometric luminosity ratio of the M 34 sample stars is in good agreement with the saturation limit ( $L_X/L_{\text{bol}} \approx 0.5\text{--}1.26 \times 10^{-3}$ ) derived by Pizzolato et al. (2003). For the Rossby number included between 0.1 and 0.6, the X-ray to bolometric luminosity ratio of the sample stars is still contained within the  $L_X/L_{\text{bol}}$  vs.  $Ro$  domain described by Pizzolato et al. (2003), but is spread over two orders of magnitude. In this range, the low-mass stars  $M < 0.9 M_{\odot}$  have an X-ray luminosity ratio ( $L_X/L_{\text{bol}} = 0.45 \pm 0.28 \times 10^{-3}$ ) close to the saturation limit and therefore significantly larger than that ( $L_X/L_{\text{bol}} = 0.053 \pm 0.031 \times 10^{-3}$ ) of the high-mass stars ( $M > 0.9 M_{\odot}$ ). Within these stellar groups, no correlation is

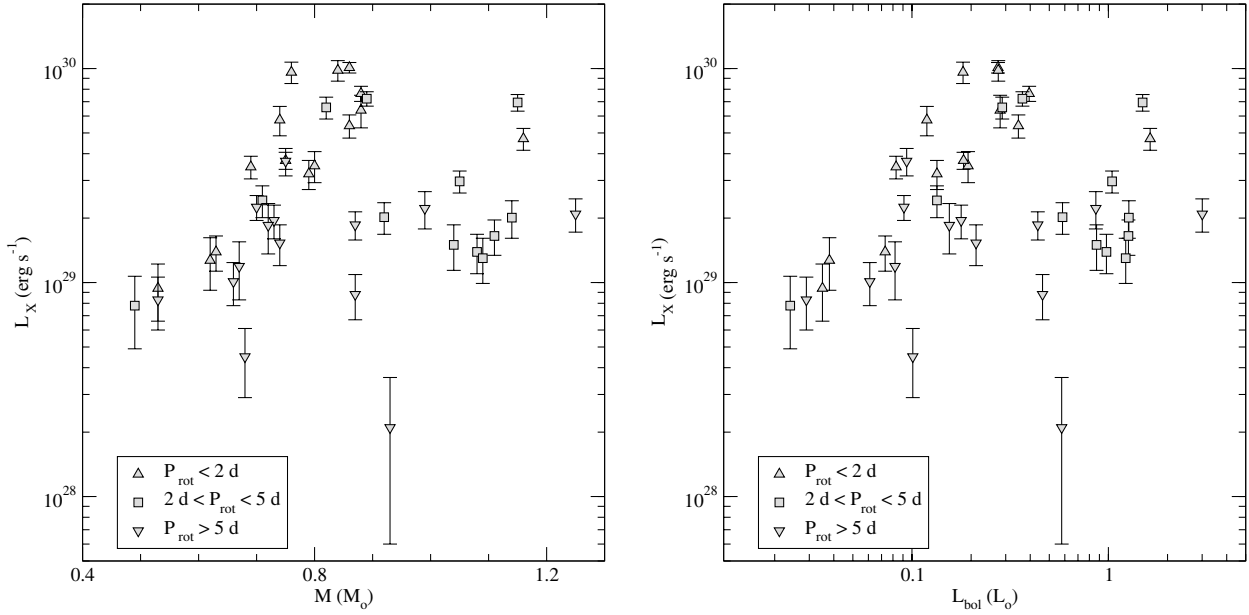


**Fig. 8.** X-ray luminosities of the M 34 sample stars vs. masses (*left*) and bolometric luminosities (*right*). Fast, medium, and slow rotators are indicated by a triangle up, a rectangle, and a triangle down, respectively.

found between X-ray to bolometric luminosity ratio and Rossby number.

The distribution of the X-ray luminosity and X-ray to bolometric luminosity ratio of the M 34 sample stars as a function of rotation period and the Rossby number is thus broadly in line with the saturated and non-saturated region of X-ray coronal emission observed by various authors (e.g., Micela et al. 1985; Vilhu 1984; Vilhu & Walter 1987; Fleming et al. 1993; Stauffer et al. 1994; Randich et al. 1996). However, the X-ray activity in M 34 does not seem to be influenced by the rotation rate alone.

### 3.5. X-ray emission vs. mass in M 34

For Rossby numbers greater than 0.1, mass seems to play a significant role in determining the magnetic activity level since low-mass stars have an X-ray to bolometric luminosity ratio significantly larger than that of high-mass stars. The dependence of X-ray luminosity on mass and bolometric luminosity is illustrated in Fig. 8. Interestingly, this dependence shows two branches, i.e., a branch where X-ray luminosity increases steeply with mass (and bolometric luminosity) and a branch where the increase of X-ray luminosity with mass (and bolometric luminosity) is softer. Stars are found in these two branches independently of their rotation rate. Such a dependence of X-ray activity on mass in M 34 has to be interpreted with care because stellar mass on the main sequence is correlated with various stellar parameters, including, e.g., bolometric luminosity and convective turnover time.

### 3.6. X-ray emission in M 34 and rotation sequences

Recent studies have shown (e.g., Barnes 2003a; Meibom et al. 2009; 2011) that young stars tend to group into two main sub-populations that lie on narrow sequences in diagrams where the measured rotation periods of the members of a stellar cluster are plotted against their  $B - V$  colors. One sequence, called the I-sequence, consists of stars that form a diagonal band of increasing period with increasing  $B - V$  color. In young clusters,

another sequence of ultra-fast rotators called the C-sequence, is also observed, bifurcating away from the I-sequence towards shorter rotation periods. Some stars lie in the intervening gap between the I- and C-sequences.

Barnes (2003b) argued that the I-sequence is related to the existence of a radiative/convective interface and can be associated with an interface dynamo, thus connecting solar-type stars and the Sun where the tachocline at the base of the convection zone is widely believed to be the source of the dynamo (Hughes et al. 2007, and references therein). The C-sequence, on the contrary, continues past the stellar mass range where full convection sets in and must be associated with a convective or turbulent dynamo discussed, for example, by Durney et al. (1993). The M 34 sample stars with known X-ray luminosities and rotational periods enable a meaningful test of the above statements.

Using the  $(B - V)_0$  color indices (see Table 1) and the rotation periods (see Table 2), I classified the M 34 sample stars in terms of the paradigm advanced in Barnes (2003a), i.e., as lying on the convective sequence (C-), on the interface sequence (I-), or in the rotational gap (g) between these sequences. The result is shown in Fig. 9 which plots the rotational periods  $P_{\text{rot}}$  of the sample stars as a function of their reddening corrected  $(B - V)_0$  indices. When unknown, the  $(B - V)_0$  index was estimated from the  $(V - I)$  index using a linear interpolation calibrated on M 34 sample stars having both color indices known.

The color-period diagram in Fig. 9 also displays the rotational isochrones of the I-sequence and of the C-sequence. Their functional forms were first introduced by Barnes (2003a). For the I-sequence, I used the form subsequently modified by Barnes (2007) in line with the gyrochronology analysis of M 34 performed by M 11. The equations of these isochrones are as follows:

$$P_C = 0.2 \exp([(B - V)_0 + 0.1 - t/3000]^3 \times t/100) \quad (3)$$

$$P_I = [a \times ((B - V)_0 - b)^c] \times t^n \quad (4)$$

where  $a = 0.730$ ,  $b = 0.481$ , and  $c = 0.532$  are the coefficients determined from a least squares fit of  $P_I(t, B - V)$  to the M 34 I sequence using  $n = 0.52$  and  $t = 220$  Myr (M 11). The

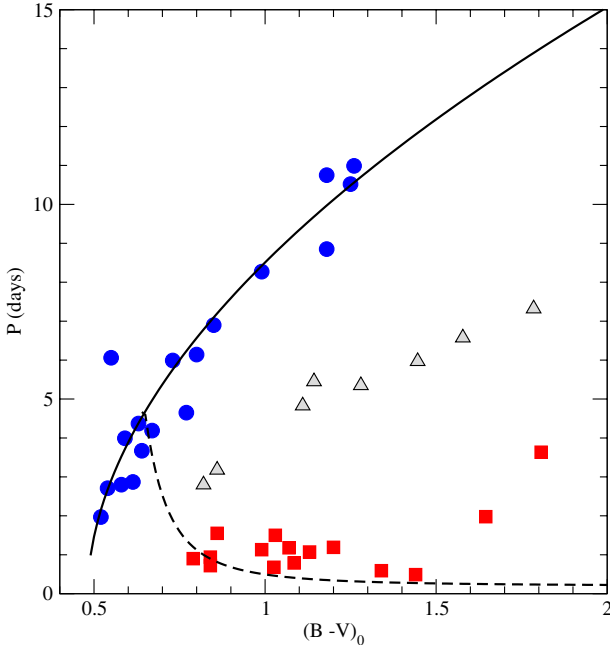


**Fig. 9.** Rotation periods vs.  $(B - V)_0$  indices of the M 34 sample stars. The solid line represents the I sequence defined by Barnes (2007). The dashed line represents the C sequence determined by Meibom et al. (2011). M 34 stars represented as blue circles belong to the I sequence. M 34 stars represented as red square belong to the C sequence. Grey triangles represent M 34 gap stars assumed to be evolving from the C-sequence towards the I-sequence.

value  $n = 0.52$  had been previously determined by demanding solar rotation at solar age using the I-sequence from multiple young open clusters (Barnes 2007). The proximity of the M 34 data points to these curves was used to determine their membership to the I-sequence, C-sequence or the gap between them. The IgC classification of the M 34 sample stars is given in the last column of Table 2.

Figure 10 displays the X-ray to bolometric luminosity ratio of the M 34 sample stars as a function of mass distinguishing members of the I-sequence, C-sequence, and the gap. Remarkably, Fig. 10 indicates that the two branches detected previously in the  $L_X$  vs.  $M$  and  $L_X$  vs.  $L_{bol}$  diagrams (see Sect. 3.3) are closely related to the IgC classification. Indeed, members of the C-sequence and the gap have an X-ray to bolometric luminosity ratio that is constant and close to the  $10^{-3}$  saturation level. This ratio is significantly lower and decreases slightly as a function of mass on the I-sequence.

Figure 11 displays the X-ray luminosity vs. rotation period diagram (left) and the X-ray to bolometric luminosity ratio vs. Rossby number diagram (right) of the M 34 sample stars, distinguishing members of the I-sequence, C-sequence and the gap. Figure 11 confirms the existence of a correlation between the X-ray activity regimes and the IgC rotation sequence classification. Indeed, members of the C-sequence have short rotation periods ( $P_{rot} < 2$  days), small Rossby numbers ( $Ro < 0.1$ ), and an X-ray to bolometric luminosity level close to the  $10^{-3}$  saturation level. Members of the I-sequence, in contrast, have a slower rotation ( $P_{rot} \geq 2$  days), larger Rossby numbers ( $Ro \geq 0.17$ ), and an X-ray to bolometric luminosity ratio significantly smaller than the saturation limit.

Interestingly, gap stars occupy an intermediary position in the  $L_X$  vs.  $P_{rot}$  and  $L_X/L_{bol}$  vs.  $Ro$  diagrams. On the one hand, gap stars have rotation periods ( $P_{rot} \geq 2$  days) and the Rossby

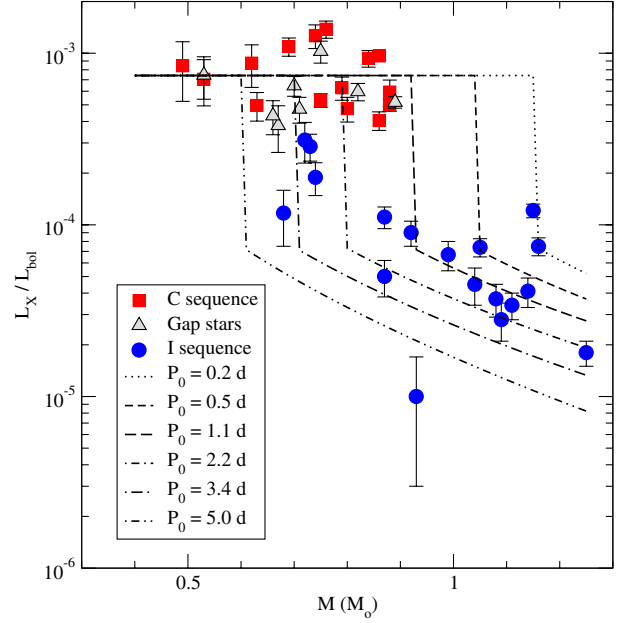


**Fig. 10.** X-ray to bolometric luminosity ratios of the M 34 sample stars vs. masses compared with an X-ray luminosity model of 220 Myr stars with initial rotation periods on the ZAMS ranging from 0.2 to 5.0 days. Stars represented as blue circles are members of the I-sequence. Stars represented as blue square belong to the C-sequence. Triangles represent gap stars assumed to be evolving from the C-sequence towards the I-sequence.

number ( $Ro \geq 0.17$ ) in the same range as those of I-sequence stars. They would therefore be expected to operate in a non-saturated regime of X-ray emission. On the other hand, their X-ray to bolometric luminosity ratio is similar to those of C-sequence stars, i.e., close to the saturation level.

Although the Rossby number and the X-ray to bolometric luminosity ratio are key parameters that differentiate the C-sequence from the I-sequence and from the gap, stars in these groups do not exhibit any correlation between X-ray activity and rotation. Instead, their X-ray luminosity seems to depend on bolometric luminosity or stellar mass.

#### 4. A model of X-ray activity evolution

The C/I dichotomy for stellar rotation was recently formulated mathematically by Barnes (2010) in a simple model that describes the rotational evolution of cool stars on the main sequence. According to this model, the time evolution of the rotational period of a main-sequence star depends on two parameters, (i) its initial period of rotation  $P_0$  on the zero-age main sequence (ZAMS) and (ii) its convective turnover time. The parameter  $P_0$ , in fact, enters as a constant of integration in the solution of a differential equation. These parameters are related by the following expression (Barnes 2010):

$$t = \frac{\tau_{c,B}}{k_C} \times \ln\left(\frac{P(t)}{P_0}\right) + \frac{k_I}{2\tau_{c,B}} \times (P(t)^2 - P_0^2), \quad (5)$$

where the constants  $k_C = 0.646$  days Myr $^{-1}$ ,  $k_I = 452$  Myr day $^{-1}$ , and  $\tau_{c,B} = 34.884$  days have been calibrated on the Sun, with input from open-cluster rotation observations demanding that the rotation of the star start off with an initial period of 1.1 days and be 26.09 days at an age of 4570 Myr (Barnes 2010). I combined

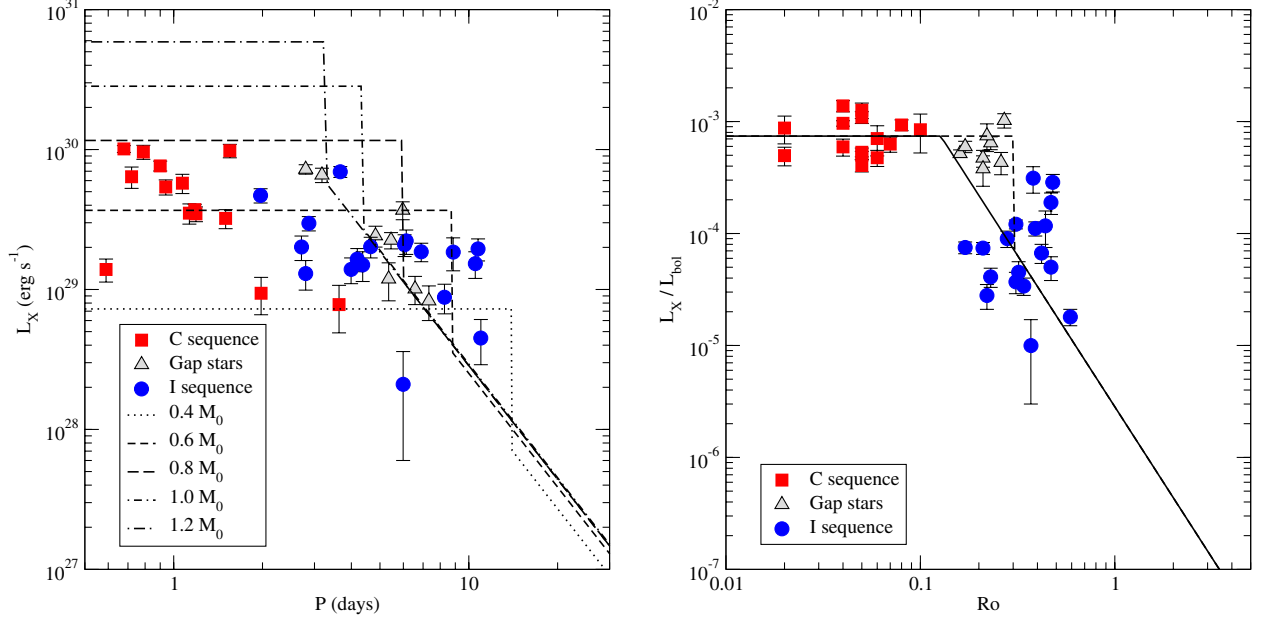


**Fig. 11.** *Right:* X-ray to bolometric luminosity ratios of M34 sample stars vs. Rossby numbers. The solid line represents the rotation-activity relationship derived by Wright et al. (2011), and the dashed line represents the X-ray evolution model set-up in the present study based on M34 data. *Left:* X-ray luminosities vs. rotation periods of M34 stars compared with this X-ray evolution model for stellar masses in the range  $0.4 \leq M/M_{\odot} \leq 1.2$ . In both graphs, M34 stars represented as red squares belong to the C sequence. M34 stars represented as blue circles are members of the I sequence. Triangles represent M34 gap stars assumed to be evolving from the C sequence towards the I sequence.

the above expression with the unique mass-independent prediction of the X-ray emission level (Pizzolato et al. 2003; Wright et al. 2011), expressed as follows:

$$\frac{L_X}{L_{\text{bol}}} = \begin{cases} R_{X,\text{sat}} & \text{if } P(t)/\tau_c < Ro^{\text{sat}} \\ C^{\text{st}} \times (\tau_c/P(t))^{\beta} & \text{if } P(t)/\tau_c \geq Ro^{\text{sat}}. \end{cases} \quad (6)$$

In this equation,  $Ro^{\text{sat}}$  is the Rossby number below which the saturation of X-ray emission occurs, and  $R_{X,\text{sat}}$  is the saturation level of the X-ray to bolometric luminosity ratio. Both  $Ro^{\text{sat}}$  and  $R_{X,\text{sat}}$  are independent of stellar mass. The combination of Eqs. (5) and (6) constitutes a simple time evolution model of the X-ray luminosity of main-sequence stars as a function of the stars' convective turnover time and initial period of rotation  $P_0$  on the ZAMS. The dependence on mass of the stellar X-ray luminosity is defined by the parameterization of the bolometric luminosity and convective turnover time as a function of stellar mass.

Following Wright et al. (2011), I used a mean saturation level  $R_{X,\text{sat}} = 0.74 \times 10^{-3}$  and a slope  $\beta = 2.7$  that provides a better fit to the Sun's X-ray luminosity. In Eq. (6), I also used the empirical relationship between the convective turnover time and the stellar mass proposed by these authors (see Eq. (2)). However, in Eq. (5), I rescaled the turnover time mass dependence of Wright et al. (2011) by a factor  $(\tau_{c,B}/\tau_{c,W})_{\odot} \approx 2.4$  to correct for the different value of the Sun convective turnover time used by Barnes (2010). The proportionality coefficient  $C^{\text{st}}$  in Eq. (6) was estimated using solar data as follows:

$$C^{\text{st}} = (L_{X,\odot}/L_{\odot}) \times (P_{\odot}/\tau_{c,\odot})^{\beta}, \quad (7)$$

with  $\log(L_{X,\odot}/L_{\odot}) = -6.24$  (Judge et al. 2003),  $P_{\odot} = 26.09$  days (Donahue et al. 1996), and  $\tau_{c,\odot} = 14.45$  days (Wright et al. 2011). The stellar mass and bolometric luminosity on the main sequence were related by the expression (e.g., Duric 2003)

$$(M/M_{\odot}) = (L_{\text{bol}}/L_{\odot})^{4.0}. \quad (8)$$

Regarding the critical Rossby number  $Ro^{\text{sat}}$  at which X-ray emission saturates, I initially used the value  $Ro^{\text{sat}} = 0.13$  derived by Wright et al. (2011) from their study of a large stellar sample which includes members of IC 2602 (~30 Myr), IC 2391 (~30 Myr), NGC 2547 (~40 Myr),  $\alpha$  Persei (~50 Myr), Pleiades (~125 Myr), NGC 2516 (~150 Myr), Praesepe (~580 Myr), Hyades (~625 Myr), and field stars. This value leads to a continuous transition from saturated to non-saturated X-ray emission with decreasing Rossby number. Figure 11 (right) shows that this model provides good estimates of the X-ray to bolometric luminosity ratios of M34 C-sequence stars with a Rossby number lower than 0.1 and of X-ray faint M34 I-sequence stars. However, X-ray bright I-sequence stars and gap stars in M34 have an  $L_X/L_{\text{bol}}$  ratio significantly higher than the  $L_{X,\odot}/L_{\odot}$  vs.  $Ro$  parametrization by Wright et al. (2011).

A critical Rossby  $Ro^{\text{sat}} = 0.3$  provides a better fit to the  $L_X/L_{\text{bol}}$  vs.  $Ro$  curve in M34, as illustrated by the dashed curved in Fig. 11 (right). This modification only affects the activity-rotation relationship derived by Wright et al. (2011) in a narrow range of Rossby numbers included between 0.13 and 0.3. Due to the dispersion of the data points, it remains consistent with the  $L_X/L_{\text{bol}}$  vs.  $Ro$  plot of statistical data derived from rotation periods and X-ray luminosities observations on main-sequence stars in many open clusters (see Fig. 2 in Wright et al. 2011). One major difference, however, is that the transition between the saturated and non-saturated regimes of X-ray emission is not smooth. It appears as a decrease of the X-ray to bolometric luminosity ratio by about one order of magnitude at  $Ro^{\text{sat}} = 0.3$  (see Fig. 11 right).

## 5. X-ray emission in M34 vs. X-ray activity model

Using the above model, I calculated the X-ray luminosity as a function of rotation periods for main-sequence stars with masses in the range  $0.4 \leq M/M_{\odot} \leq 1.2$  (see Fig. 11 left-hand side). By construction, the model reproduces features observed by

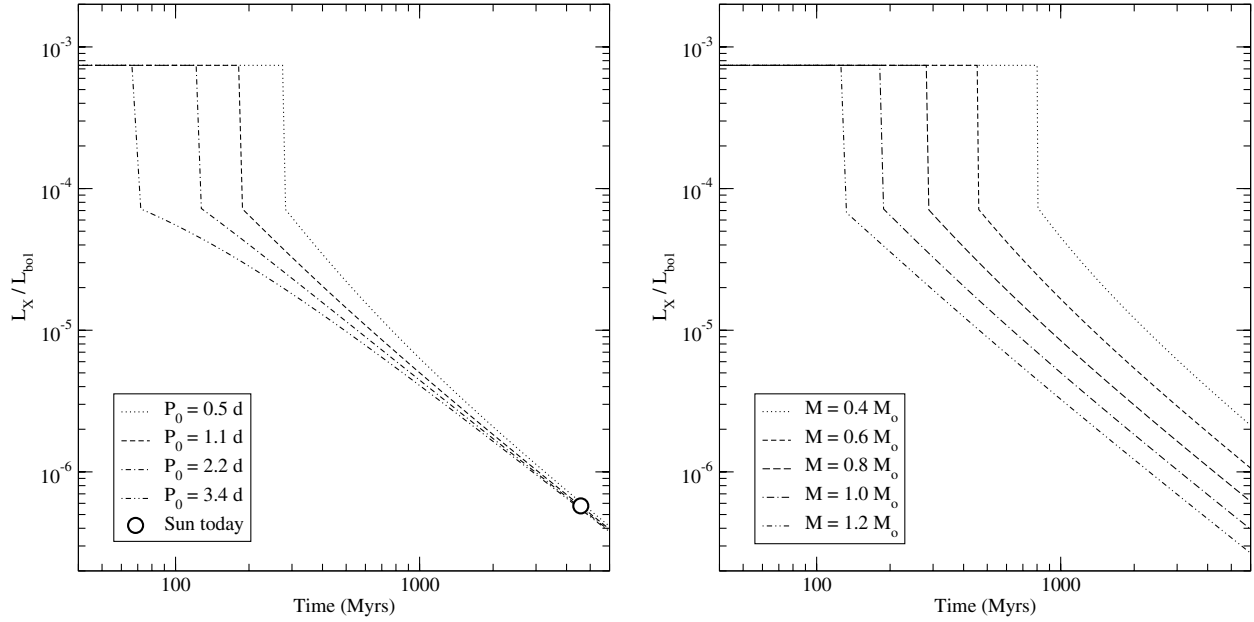


**Fig. 12.** *Left:* time evolution of the X-ray to bolometric luminosity ratio of a Sun-like star with different initial rotation periods on the ZAMS. *Right:* time evolution of the X-ray to bolometric luminosity ratio of main-sequence stars with masses in the range  $0.4 \leq M/M_{\odot} \leq 1.2$  for an initial rotation period  $P_0 = 1.1$  d on the ZAMS.

Pizzolato et al. (2003) in their study on the relationship between coronal X-ray emission and stellar rotation in late-type main sequence stars. In particular, it shows that, (i) the parameterization of the X-ray activity-rotation relationship in terms of  $L_X$  vs.  $P_{\text{rot}}$  instead of  $L_X/L_{\text{bol}}$  vs.  $Ro$  considerably increases the scatter of data points due to the introduction of a mass dependence; (ii) the X-ray luminosity saturation level increases with stellar mass due to the strong mass dependence of the bolometric luminosity; and (iii) the rotation period at which saturation occurs is proportional to the critical Rossby number and increases with decreasing stellar mass since the convective turnover time is a decreasing function of stellar mass.

Using a critical Rossby number  $Ro^{\text{sat}} = 0.3$ , I calculated the time evolution of the X-ray luminosity of Sun-like stars for different initial rotation periods on the ZAMS. The results are shown in Fig. 12 (left-hand side) for a range of rotation periods observed in young stellar clusters. This calculation indicates that Sun-like stars with initial rotation period on the ZAMS in the range 0.5 to 3.4 days experience a transition from a saturated to a non-saturated regime of X-ray emission at ages between about 70 and 300 Myr. Figure 12 (right-hand side) shows the calculated time evolution of the X-ray luminosity of late-type stars with masses in the range  $0.4 \leq M/M_{\odot} \leq 1.2$  for a 1.1 day initial rotation period on the ZAMS. For stars with masses ranging from  $0.8 M_{\odot}$  to  $1.2 M_{\odot}$ , the transition occurs at ages between 100 Myr and 300 Myr. The absence of any clear rotation-activity relationship in M 34 would be explained by the fact that M 34 Sun-like stars are evolving from a saturated to a non-saturated regime of X-ray emission, while lower mass M 34 stars still operate in a saturated regime of X-ray emission. It appears that cool stars of a fixed age such as in M 34 sprawl across the divide between saturated and non-saturated X-ray emission and that an X-ray activity vs. rotation relationship only appears once stars have made the transition to the I-rotation sequence.

In order to understand the mass or bolometric luminosity dependence of the X-ray emission that is instead observed in M 34, I used the above model to calculate the X-ray to bolometric

luminosity ratio of late-type stars at an age of 220 Myr as a function of their mass. The curves obtained for different initial rotation periods on the ZAMS are compared with M 34 stars in Fig. 10. The X-ray to bolometric luminosity model only depends on the Rossby number, which is time dependent since stellar rotation decreases with time due to rotational braking by stellar winds. Hence the distribution of  $L_X/L_{\text{bol}}$  vs. mass in a given cluster results from the rotational period distribution of the stars at the corresponding age relative to their convective turnover time. The rotational period of each star at a given time depends on its initial value on the ZAMS and on its convective turnover time.

I calculated the rotation period and Rossby number of late-type stars at an age of 220 Myr as a function of their initial rotation period on the ZAMS using the rotation evolution model introduced by Barnes (2010) but scaled to the calibration value of the Sun convective turnover time used by Wright et al. (2011). The results are displayed in Fig. 13. They indicate that stars with  $0.4 \leq M/M_{\odot} \leq 1.2$  and  $0.2 \text{ days} \leq P_0 \leq 5.0 \text{ days}$  shall have rotation periods included between 0.7 and 9 days in line with the mass and rotation period distribution (see Fig. 5) of the M 34 stellar sample. The Rossby number calculation results indicate that, at the age of M 34, all stars with stellar mass lower than  $0.6 M_{\odot}$  shall have a Rossby number lower than the critical value and therefore operate in a saturated regime of X-ray emission, as observed in M 34. The model also indicates that no star with a mass higher than that of the Sun shall operate in the saturation regime unless its initial rotation period on the ZAMS is lower than about 0.7 days. No such stars are observed in M 34. The model of rotation evolution introduced by Barnes (2010) thus explains that M 34 Sun-like stars with masses in the range  $0.6 \leq M/M_{\odot} \leq 1.0$  evolve close to the transition between two regimes of X-ray emission at a Rossby number of 0.3 when using the turnover time calibration of Wright et al. (2011).

## 6. Discussion

In the present paper, I report on the study results of a sample of 220 Myr old stars with known X-ray luminosities and

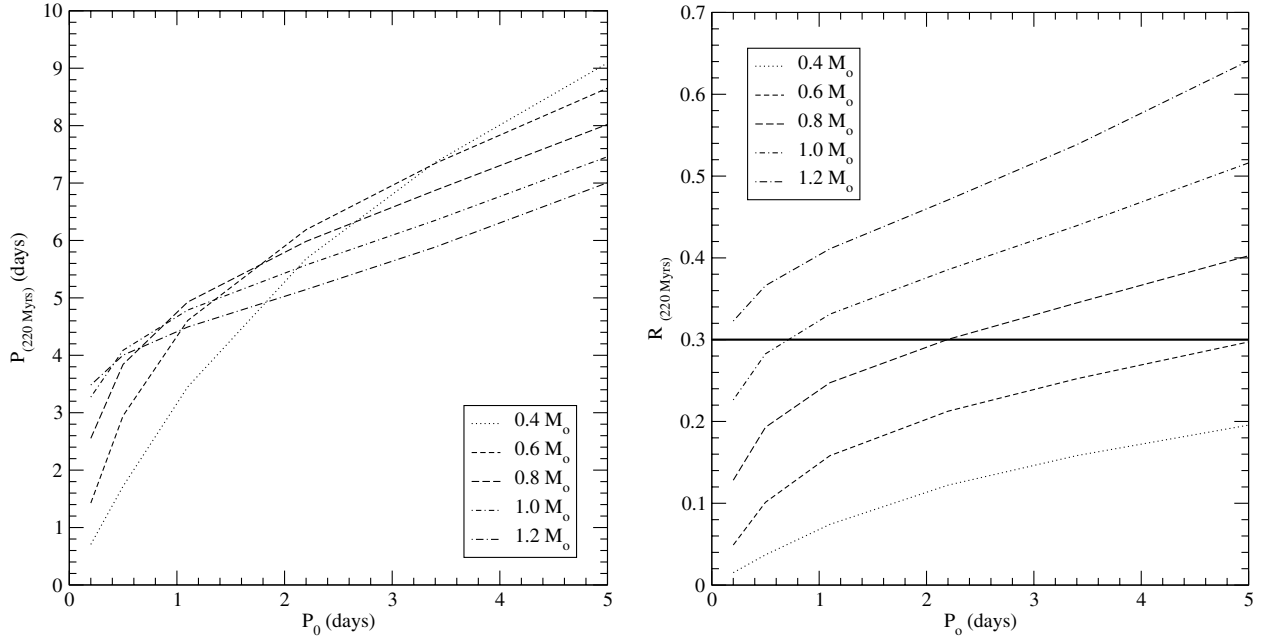


**Fig. 13.** *Left:* rotation periods of late-type stars at an age of 220 Myr as a function of their initial rotation period on the ZAMS calculated using the rotation evolution model introduced by Barnes (2010). *Right:* Rossby number of late-type stars at an age of 220 Myr as a function of their initial rotation period on the ZAMS calculated with the same model but scaled to the calibration value of the Sun convective turnover time used by Wright et al. (2011). The horizontal line shows the critical Rossby number, which separates the saturated regime (at low Rossby number) from the non-saturated regime of X-ray emission.

rotation periods. This sample was obtained by correlating the *XMM-Newton* Serendipitous Source Catalog with lists of M 34 cluster members having known rotation periods. The mass distribution of the 41 sample stars spreads between 0.4 and 1.3  $M_{\odot}$ .

The X-ray luminosity distribution of M 34 stars in a  $\log L_X$  vs.  $\log P$  diagram is broadly in line with the X-ray emission from late-type cluster stars that delineate two kinds of dependences on stellar rotation (Patten & Simon 1996; Randich 2000; Feigelson et al. 2003). Indeed, fast rotators in M 34 show a relative constancy of their X-ray emission at a high level regardless of rotation speed, and their X-ray to bolometric luminosity ratio is in good agreement with the  $(L_X/L_{\text{bol}}) \approx 10^{-3}$  saturation level derived by Pizzolato et al. (2003) from the observation of many field stars and open clusters members.

For slower rotators in M 34, a decline of X-ray emission is observed but without any correlation between X-ray luminosity and rotation period. For these stars, no correlation is found between their X-ray to bolometric luminosity ratios and the Rossby number, although the dispersion of M 34 data points in the  $L_X/L_{\text{bol}}$  vs.  $Ro$  graph is much lower than in the  $L_X$  vs.  $P_{\text{rot}}$  graph. Instead, the present study shows that a correlation exists between the saturated and non-saturated regime of X-ray emission and the rotational sequences that have been observed in M 34 (J10; M11) and other open clusters (e.g., Meibom et al. 2009; Hartman et al. 2010; Irwin et al. 2009).

Indeed, the rotation periods of late-type stars in M 34 trace two distinct rotational sequences in a color-period diagram, i.e., a fast (C) rotational sequence and a moderate-to-slow (I) rotational sequence. M 34 members of the C-sequence are emitting in the so-called saturated regime of X-ray emission, while M 34 stars of the I-sequence are located in the non-saturated X-ray emission regime of the  $L_X/L_{\text{bol}}$  vs.  $Ro$  diagram. M 34 stars located in the gap between the C- and the I-sequences occupy an intermediary position in this diagram. They have rotation periods and Rossby number in the same range as those of the I-sequence stars, but emit X-rays as C-sequence stars, i.e., close

to the saturation level. M 34 sample stars in these three rotational groups, in particular those on the I-sequence associated with the non-saturated regime of X-ray emission, do not follow any X-ray emission vs. rotation relationship. Instead, a parameter correlated with mass or bolometric luminosity seems to play a key role in controlling their level of magnetic activity.

Correlations between rotation sequences and X-ray emission regimes were searched by Barnes (2003b) in four groups of stars including IC 2391 (~30 Myr), IC 2602 (~30 Myr),  $\alpha$  Persei (~50 Myr), and a group of field M dwarfs from James et al. (2000). Barnes (2003b) argued that the X-ray observation of cluster and field stars has a three-segmented morphology because there are three kinds of rotating stars. He associated the presence of stars on the rotational I-sequence with unsaturated X-ray emission and suggested that stars in the gap between the C- and I-sequences show saturated emission in agreement with the present M 34 study. However, he concluded that stars on the C-sequence were coronally supersaturated, which is clearly not the case in M 34, where no sample star is found in a supersaturated regime and where rapidly rotating star members of the C-sequence are all emitting in the X-ray saturation regime.

The association of supersaturated coronal emitters with stars on the C-sequence was also argued against by Wright et al. (2011), based on the very small number of supersaturated X-ray emitters compared to the much larger number of fast rotators found on the C-sequence of young clusters. Using a large stellar sample that included members of IC 2602, IC 2391, NGC 2547 (~40 Myr),  $\alpha$  Persei, Pleiades (~125 Myr), NGC 2516 (~150 Myr), Praesepe (~580 Myr), Hyades (~625 Myr), and field stars, Wright et al. (2011) also noted that stars with saturated X-ray emission are found on the C-sequence of fast rotators, while those with non-saturated emission can be found on the I-sequence of slow rotators. However, these authors did not associate stars in the gap between the C- and I-sequences with any specific X-ray emission regime.

The C/I dichotomy for stellar rotation was recently formulated mathematically by Barnes (2010) in a simple model that describes the rotational evolution of cool stars on the main sequence. By combining this model with the formulation of X-ray emission as a function of the Rossby number proposed by Pizzolato et al. (2003), I constructed a time evolution model of the X-ray luminosity of late-type stars on the main sequence.

Using the rotation-activity parametrization calibrated on the Sun and with statistical data derived from X-ray luminosity and rotational periods measurements (Wright et al. 2011) in many open clusters, I obtained a model validated on a huge sample of main-sequence stars that include members of IC 2602, IC 2391, NGC 2547,  $\alpha$  Persei, Pleiades, NGC 2516, Praesepe, Hyades, and field stars. By comparing this X-ray activity evolution model with X-ray emission in M 34, I found that a critical Rossby  $Ro^{\text{sat}} = 0.3$  provides a better fit to the  $L_X/L_{\text{bol}}$  vs.  $Ro$  curve in M 34 than the value  $Ro^{\text{sat}} \approx 0.16 \pm 0.02$  obtained by Wright et al. (2011). Incorporating this modification, the model not only reproduces the relationship between coronal X-ray emission and stellar rotation observed by many authors among late-type main sequence stars, it also accounts for the sharp transition from a saturated to a non-saturated regime of X-ray emission observed among Sun-like stars in M 34.

The physical significance of this transition between X-ray emission regimes is not clear. It has been suggested that this phenomenon is caused by a saturation of the dynamo (e.g., Vilhu 1984), a saturation of the filling factor of active regions on stellar surfaces (Vilhu 1984), or a centrifugal stripping of the corona at high rotation rates (Jardine & Unruh 1999). The detections of rotational modulation in M 34 saturated stars argue against an explanation by a saturation of the filling factor of active regions on the surfaces of rapidly rotating stars. Wright et al. (2011) argued that centrifugal stripping is also unlikely to be responsible for X-ray saturation since the theoretical form of constant corotation radius in the mass-rotation diagram is notably different from the empirically derived form of the saturation boundary.

The hypothesis of a saturation of the dynamo itself is not supported by the present study of M 34 either. A saturation of the dynamo itself would imply a continuous evolution and smooth transition of the dynamo efficiency from a regime of steadily increase of the  $L_X/L_{\text{bol}}$  ratio with decreasing Rossby number up to a plateau of relative constancy. Instead, M 34 sample stars show a steep transition in X-ray to bolometric luminosity ratio between the C-sequence and gap stars that emits close to the  $10^{-3}$  saturation level, and the I-sequence stars, whose  $L_X/L_{\text{bol}}$  ratio is significantly lower for similar values of the Rossby number. This suggests a transition between two different dynamo regimes.

Indeed, the  $L_X/L_{\text{bol}}$  ratio can be considered as an indicator of the dynamo efficiency. The bolometric luminosity is a close upper limit of the total outer convective flux since almost all the energy is transported by convection in the top layers of the outer convection zone (e.g., Böhm-Vitense 1992). The coronal X-ray radiative flux density is proportional to the average surface magnetic flux density (Fisher et al. 1998). Hence, the  $L_X/L_{\text{bol}}$  ratio is a lower limit of the ratio between the surface magnetic flux and the outer convective flux. The decrease of this ratio by one order of magnitude observed in M 34 around Rossby numbers of 0.3 is thus indicative of a significant change in dynamo efficiency that could be the result of a dynamo regime transition. The interpretation of the  $L_X/L_{\text{bol}}$  ratio as a dynamo efficiency indicator is supported by measurements of magnetic fields (Reiners et al. 2009) that saturate on rapidly rotating M dwarf in the same regime as saturation of coronal and chromospheric emission.

The association of the two X-ray emission regimes with two different dynamos was explored by Wright et al. (2011). These authors suggested that the saturated and non-saturated X-ray emissions are just the manifestation of two different dynamos, i.e., a turbulent dynamo on the C-sequence parameterized by the bolometric luminosity and a cyclic, interface-type dynamo on the I-sequence parameterized by the Rossby number. This interpretation is supported by the steep transition in X-ray to bolometric luminosity ratio observed in the M 34 open cluster. However, the hypothesis of a transition to a solar-type interface-dynamo is not corroborated by M 34 stars located on the I-sequence since no relationship is observed between their X-ray to bolometric luminosity ratio and their Rossby number. Such a correlation may not have been detected because the range in Rossby numbers of I-sequence stars in M 34 is narrow ( $0.17 \leq Ro \leq 0.59$ ) and the dispersion of their X-ray to bolometric luminosity is large ( $0.01 \leq L_X/L_{\text{bol}} \leq 0.30$ ), possibly due to a large variability of their X-ray activity. The present study suggests that this correlation is not observed in M 34 because some of its I-sequence stars are still in a transition between the saturated and non-saturated regimes of X-ray emission. This transition, indeed, occurs after stars reach the I-sequence since gap stars are still in a regime of saturated X-ray emission.

Using Eq. (6) with  $P(t_{\text{sat}}) = Ro^{\text{sat}} \times \tau_{c,B}$ , it is possible to estimate the age  $t_{\text{sat}}$  at which the X-ray emission of a star changes from the saturated to the non-saturated regime:

$$t_{\text{sat}} = \frac{\tau_c}{k_C} \times \ln \left( \frac{Ro^{\text{sat}} \times \tau_c}{P_0} \right) + \frac{k_I}{2\tau_c} \times \left( (Ro^{\text{sat}} \times \tau_c)^2 - P_0^2 \right). \quad (9)$$

This age  $t_{\text{sat}}$  is plotted in Fig. 14 (left-hand side) as a function of mass for a range of initial rotation periods on the ZAMS typical of those observed in young open clusters. This age can be compared with the age  $t_{\text{gap}}$  (see Eq. (26) in Barnes 2010) taken by a star to evolve through its C-rotation phase, and reach the nominal rotational gap,  $g$ , marking the onset of the I-rotation phase. The comparison shows that  $t_{\text{sat}} \gg t_{\text{gap}}$  for all stars, indicating that the transition from a saturated to a non-saturated regime of X-ray emission, occurs well after the stars have reached the I-rotational sequence.

The change of X-ray emission regime, possibly resulting from a dynamo regime transition, is thus posterior to the stellar evolution through the rotational gap between the C- and I-sequences, which corresponds to a maximum of the rotation deceleration attributed to magnetic braking by coronal winds. Remarkably, the delay  $t_{\text{sat}} - t_{\text{gap}}$  between the change of emission regime and the arrival on the I-sequence is independent of the initial rotational period on the ZAMS and can be expressed as follows:

$$t_{\text{sat}} - t_{\text{gap}} = \frac{\tau_c}{k_C} \times \left( \ln \left( Ro^{\text{sat}} \sqrt{k_I k_C} \right) + \frac{k_I k_C Ro^{\text{sat}2}}{2} - 1 \right). \quad (10)$$

According to the model, this delay ranges from  $\sim 100$  Myr at  $M = 1.2 M_{\odot}$  to 430 Myr at  $M = 0.4 M_{\odot}$  (see Fig. 14 right-hand side). It is proportional to the convective turnover time and therefore increases with the depth of the convection zone.

The decline of stellar rotation with age on the main sequence is thought to be the result of magnetic braking due to coronal winds, but the details of this spin-down process are not understood. It has been argued that only the outer surface of a star is magnetically braked by the wind, while the interior of the star continues to spin at a faster rate (Stauffer & Hartman 1987; Stauffer et al. 1984; Pinsonneault et al. 1989). Alternatively, stars

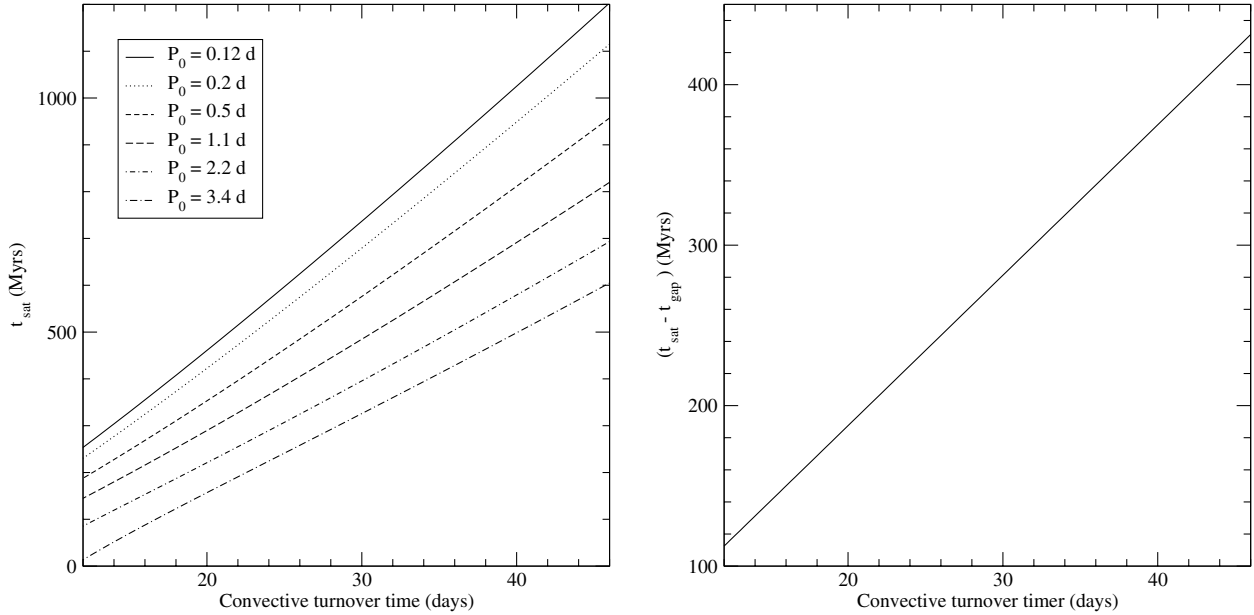


**Fig. 14.** *Left:* age  $t_{\text{sat}}$  on the main sequence at which stars change from a saturated to a non-saturated regime of X-ray emission as a function of convective turnover time using Wright et al. (2011) calibration. *Right:* time delay  $t_{\text{sat}} - t_{\text{gap}}$  between the epoch of X-ray emission regime transition and the onset of the I-rotation phase.

have been claimed to rotate as rigid bodies, owing to fluid instabilities or magnetic stresses (Mestel & Weiss 1987). Epochs of decoupling and recoupling of the stellar core and envelope have also been suggested (Stauffer et al. 1984; Soderblom et al. 1993; Jianke & Collier Cameron 1993) since the concept of decoupling, if permanent, is in conflict with helioseismic observations of the Sun as solid-body rotator (Gough 1982; Duvall et al. 1984; Goode et al. 1991; Eff-Darwich et al. 2002).

In line with this hypothesis, Barnes (2003a) proposed that the C-sequence is due to the coupling of the stellar wind to just the convective zone that is decoupled from the radiative zone, while the I-sequence is due to the coupling of the wind with the entire star. The transition across the gap between these two rotation sequences would therefore be associated with a coupling between the radiative and the convective zone. Barnes (2003) suggested that stars on the convective sequence generate a convective or turbulent dynamo similar to that described by Durney et al. (1993). He proposed that the shear between the fast spinning radiative interior and the convective envelope would eventually generate an interface dynamo that results in the transition onto the I-sequence.

According to the current picture of such an interface dynamo, the large scale toroidal magnetic field responsible for the formation of active regions is amplified and stored at the base of the convection zone (e.g., Gilman 2000; Charbonneau 2010). Following the Barnes (2003a) scenario, a delay would thus be expected for the active region flux tubes to rise from the base of the convection zone to the stellar surface after the onset of the interface dynamo. Solar cycle dynamo models suggest that the toroidal magnetic field at the base of the solar convection zone is of the order of 40–50 kG with typical rise time of the order of a couple of years (Weber et al. 2011). However, these fields may not have been initially so strong, and Parker (1975) estimated that a field of 10 kG in a rising tube of  $10^4$  km radius representing a magnetic flux comparable to the flux in a large sunspot would rise across the solar convection at a negligible rate.

The above scenario that links the transition between rotational sequences with a transition between dynamo regimes was

refuted by Barnes & Kim (2010). These authors argued that the observed transition of stars from the C- to the I-sequence is not coincident with a change of the mass dependence of these sequences from that of the convection zone alone to that of the entire star.

## 7. Summary

In the present study, I compare the X-ray luminosity distribution vs. rotation periods and Rossby numbers of a sample of M 34 late-type stars with rotation-activity relationships established on a large sample of cluster members and field stars. The distribution of X-ray luminosity in M 34 is also compared with a model of X-ray activity evolution obtained by combining the X-ray activity-rotation relationship with a recent model of stellar rotation evolution on the main sequence.

Fast rotators in M 34 show a relative constancy of their X-ray emission at a high level, regardless of rotation speed. Moreover, their X-ray to bolometric luminosity ratio is in good agreement with the  $(L_X/L_{\text{bol}}) \approx 10^{-3}$  saturation level derived from the observation of many field stars and open clusters members. For slower rotators in M 34, a decline of X-ray emission is observed but without any clear relationship between X-ray to bolometric luminosity ratios and Rossby numbers. For Sun-like stars, no relation is found between X-ray luminosities and rotation periods either.

Instead, a correlation is observed between the saturated and non-saturated regime of X-ray emission and the C- and I-rotational sequences observed in M 34 from extensive rotational periods surveys. M 34 sample stars show a steep transition in X-ray to bolometric luminosity ratio between the C-sequence and gap stars, which emits close to the  $10^{-3}$  saturation level, and the I-sequence stars, whose  $L_X/L_{\text{bol}}$  ratio is significantly lower for similar values of the Rossby number. Comparisons of the X-ray emission distributions in M 34 with an X-ray luminosity evolution model suggest that the transition between the saturated and non-saturated regime of X-ray emission occurs in

M 34 cluster members depending on their convective turnover time and initial period of rotation on the ZAMS.

I argue that the decrease of the X-ray to bolometric luminosity ratio by one order of magnitude observed in M 34 around Rossby numbers of 0.3 is indicative of a change in dynamo efficiency. The transition from the saturated to the non-saturated regime of X-ray emission among main-sequence stars would thus be the result of a dynamo regime transition, possibly between a turbulent dynamo and an interface-type dynamo. The X-ray luminosity evolution model provides an estimate of the stellar age at which this transition occurs as a function of stellar mass and initial rotation period on the ZAMS. It indicates that the time delay between the change in X-ray emission regime and the transition between rotation sequences (that corresponds to a maximum of the rotational braking by coronal winds) is proportional to the convective turnover time. However, these two phenomena may not be related.

*Acknowledgements.* I am grateful to the anonymous referee for the helpful comments that allowed me to improve the paper.

## References

- Baliunas, S. L., Donahue, R. A., Soon, W. H., et al. 1995, *ApJ*, 438, 269  
 Baraffe, I., Chabrier, G., Allard, F., & Hauschildt, P. H. 1998, *A&A*, 337, 403  
 Barnes, S. A. 2003a, *ApJ*, 586, 464  
 Barnes, S. A. 2003b, *ApJ*, 586, L145  
 Barnes, S. A. 2007, *ApJ*, 669, 1167  
 Barnes, S. A. 2010, *ApJ*, 722, 222  
 Barnes, S. A., & Kim, Y.-C. 2010, *ApJ*, 721, 675  
 Boehm-Vitense, E. 1992, *Introduction to stellar astrophysics – Stellar structure and evolution*, Vol. 3 (Cambridge University Press)  
 Canterna, R., Crawford, D. L., & Perry, C. L. 1979, *PASP*, 91, 263  
 Casagrande, L., Ramirez, I., Melendez, J., et al. 2010, *A&A*, 512, A54  
 Charbonneau, P. 2010, *Liv. Rev. Sol. Phys.*, 7, 3  
 Delorme, P., Cameron, A. C., Hebb, L., et al. 2011, in the *Proc. 16th Cambridge Workshop on Cool Stars, Stellar Systems, and the Sun*, ASP Conf. Ser., 448, 841  
 Donahue, R. A., Saar, S. H., & Baliunas, S. L. 1996, *ApJ*, 466, 384  
 Duric, N. 2003, *Advanced Astrophysics* (Cambridge University Press)  
 Durney, B. R., & Latour, J. 1978, *Geophys. Astrophys. Fluid Dyn.*, 9, 241  
 Durney, B. R., De Young, D. S., & Roxburgh, I. W. 1993, *Sol. Phys.*, 145, 207  
 Duvall, T. L., Jr., Dziembowski, W. A., Goode, P. R., et al. 1984, *Nature*, 310, 22  
 Eff-Darwich, A., Korzennik, S. G., Jimnez-Reyes, S. J., & Prez Hernandez, F. 2002, *ApJ*, 573, 857  
 Feigelson, E. D., Gaffney, J. A., Garmire, G., Hillenbrand, L. A., & Townsley, L. 2003, *ApJ*, 584, 911  
 Fisher, G., Longcope, D., Metcalf, T., et al. 1998, *ApJ*, 508, 885  
 Fleming, T. A., Giampapa, M. S., Schmitt, J. H. M. M., & Bookbinder, J. A. 1993, *ApJ*, 410, 387  
 Flower, P. J. 1996, *ApJ*, 469, 335  
 Giardino, G., Pillitteri, I., Favata, F., & Micela, G. 2008, *A&A*, 490, 113  
 Gilliland, R. L. 1985, *ApJ*, 299, 286  
 Gilman, P. A. 2000, *Sol. Phys.*, 192, 27  
 Gondoin, P. 2006, *A&A*, 454, 595  
 Gondoin, P., Aschenbach, B., Erd, C., et al. 2000, *SPIE Proc.*, 4140, 1  
 Goode, P. R., Dziembowski, W. A., Korzennik, S. G., & Rhodes, E. J., Jr. 1991, *ApJ*, 367, 649  
 Gough, D. O. 1982, *Nature*, 298, 334  
 Hartman, J. D., Bakos, G., Kovcs, G., & Noyes, R. W. 2010, *MNRAS*, 408, 475  
 Hughes, D. W., Rosner, R., & Weiss, N. O. 2007, *The Solar Tachocline* (Cambridge, UK: Cambridge University Press)  
 Ianna, P. A., & Schlemmer, D. M. 1993, *AJ*, 105, 209  
 Irwin, J., Aigrain, S., Hodgkin, S., et al. 2006, *MNRAS*, 370, 954 (I06)  
 Irwin, J., Aigrain, S., Bouvier, J., et al. 2009, *MNRAS*, 392, 1456  
 James, D. J., Jardine, M. M., Jeffries, R. D., et al. 2000, *MNRAS*, 318, 1217  
 James, D. J., Barnes, S. A., Meibom, S., et al. 2010, *A&A*, 515, A100 (J10)  
 Jansen, F., Lumb, D., Altieri, B., et al. 2001, *A&A*, 365, L1  
 Jardine, M., & Unruh, Y. C. 1999, *A&A*, 346, 883  
 Jeffries, R. D. 1999, in *Solar and Stellar Activity: Similarities and Differences*, eds. C. J. Butler, & J. G. Doyle, ASP Conf. Ser., 158, 75  
 Jeffries, R. D., Thurston, M. R., & Pye, J. P. 1997, *MNRAS*, 287, 350  
 Jianke, L., & Collier Cameron, A. 1993, *MNRAS*, 261, 766  
 Jones, B. F., & Prosser, C. F. 1996, *AJ*, 111, 1193  
 Judge, P. G., Solomon, S. C., & Ayres, T. R. 2003, *ApJ*, 593, 534  
 Kawaler, S. D. 1988, *ApJ*, 333, 236  
 Kim, Y., & Demarque, P. 1996, *ApJ*, 457, 340  
 Meibom, S., Mathieu, R. D., & Stassun, K. G. 2009, *ApJ*, 695, 679  
 Meibom, S., Mathieu, R. D., Stassun, K. G., et al. 2011, *ApJ*, 733, 115 (M 11)  
 Mestel, L., & Weiss, N. O. 1987, *MNRAS*, 226, 123  
 Meynet, G., Mermilliod, J., & Maeder, A. 1993, *A&AS*, 98, 477  
 Micela, G. 2001, in *X-ray Astronomy 2000*, eds. R. Giacconi, S. Serio, & L. Stella, San Francisco, ASP Conf. Ser., 234, 143  
 Micela, G. 2002, *Stellar Coronae in the Chandra and XMM-Newton Era*, ASP Conf. Proc., 277, 263  
 Micela, G., Sciortino, S., Serio, S., et al. 1985, *ApJ*, 292, 172  
 Micela, G., Sciortino, S., Kashyap, V., et al. 1996, *ApJS*, 102, 75  
 Micela, G., Sciortino, S., Harnden, F. R. Jr., et al. 1999, *A&A*, 341, 751  
 Mukai, K. 1993, *Legacy* 3, 21-31  
 Noyes, R. W., Hartmann, L. W., Baliunas, S. L., et al. 1984, *ApJ*, 279, 763  
 Pallavicini, R., Golub, L., Rosner, R., et al. 1981, *ApJ*, 248, 279  
 Parker, E. N. 1975, *ApJ*, 198, 205  
 Patten, B. M., & Simon, T. 1996, *ApJS*, 106, 489  
 Peres, G. 2001, in *X-ray Astronomy 2000*, ASP Conf. Ser., 234, 41  
 Perryman, M. A. C., Brown, A. G. A., Lebreton, Y., et al. 1998, *A&A*, 331, 81  
 Pinsonneault, M. H., Kawaler, S. D., Sofia, S., & Demarque, P. 1989, *ApJ*, 338, 424  
 Pizzolato, N., Ventura, P., D'Antona, F., et al. 2001, *A&A*, 373, 597  
 Pizzolato, N., Maggio, A., Micela, G., Sciortino, S., & Ventura, P. 2003, *A&A*, 397, 147  
 Randich, S. 1997, *Mem. Soc. Astron. It.*, 68, 971  
 Randich, S. 2000, in *Stellar Clusters and Association: Convection, Rotation and Dynamos*, ASP Conf. Ser., 198, 401  
 Randich, S., Schmitt, J. H. M. M., Prosser, C. F., & Stauffer, J. R. 1996, *A&A*, 305, 785  
 Reiners, A., Basri, G., & Browning, M. 2009, *ApJ*, 692, 538  
 Schatzman, E. 1962, *Ann. Astrophys.*, 25, 18  
 Schmitt, J. H. M. M. 1997, *A&A*, 318, 215  
 Schmitt, J. H. M. M., Fleming, T. A., & Giampapa, M. S. 1995, *ApJ*, 450, 392  
 Schuler, S. C., King, J. R., Fischer, D. A., et al. 2003, *AJ*, 125, 2085  
 Simon, T. 2000, *PASP*, 112, 599  
 Soderblom, D. R., Stauffer, J. R., MacGregor, K. B., & Jones, B. F. 1993, *ApJ*, 409, 624  
 Stauffer, J. R., & Hartmann, L. W. 1987, *ApJ*, 318, 337  
 Stauffer, J. R., Hartmann, L., Soderblom, D. R., & Burnham, N. 1984, *ApJ*, 280, 202  
 Stauffer, J. R., Prosser, C. F., Giampapa, M. S., Soderblom, M. S., & Simon, T. 1994, *AJ*, 106, 229  
 Stauffer, J. R., Schild, R., Barrado y Navascues, D., et al. 1998, *ApJ*, 504, 805  
 Stepien, K. 1994, *A&A*, 292, 191  
 Stern, R. A., Schmitt, J. H. M. M., & Kahabka, P. T. 1995, *ApJ*, 448, 683  
 Strüder, L., Briel, U., Dennerl, K., et al. 2001, *A&A*, 365, L18  
 Turner, M. J. L. T., Abbey, A., Arnaud, M., et al. 2001, *A&A*, 365, L18  
 Vilhu, O. 1984, *A&A*, 133, 117  
 Vilhu, O., & Walter, F. M. 1987, *A&A*, 321, 958  
 Watson, M. G., Schröder, A. C., Fyfe, D., et al. 2009, *A&A*, 493, 339  
 Weber, M. A., Fan, Y., & Miesch, M. S. 2011, *ApJ*, 741, 11  
 Wright, N. J., Drake, J. J., Mamajek, E. E., & Henry, G. W. 2011, *ApJ*, 743, 48

**Table 1.** X-ray fluxes, rotation period, and photometric index of M34 target stars.

Id. (Irwin et al.)	No. (Meibom et al.)	2XMM identifier	CR (cts/ks)	$P$ (d)	$V_0$	$(B - V)_0$	$V - I$
M34-1-2953	1	J024126.0+424814.	$1.9 \pm 0.4$	3.99	13.21	0.59	1.01
	2	J024135.1+424103.	$10.7 \pm 0.9$	0.90	14.33	0.79	
	3	J024136.6+425020.	$10.1 \pm 0.8$	2.80	14.44	0.82	
M34-4-2697	4	J024138.2+424403.	$0.3 \pm 0.2$	5.99	13.87	0.73	0.85
	5	J024138.5+423903.	$2.1 \pm 0.5$	4.37	13.36	0.63	
M34-4-2533	6	J024140.7+425446.	$1.8 \pm 0.4$	2.80	12.96	0.58	1.73
	7	J024143.9+424506.	$1.9 \pm 0.4$	0.59	16.79	1.34	
	F4-0136	J024147.3+424339.	$4.2 \pm 0.5$	2.87 (J10)	13.151	0.614	
M34-4-2412	8	J024147.8+424121.	$2.9 \pm 0.5$	6.06	11.97	0.55	1.39
M34-1-2573	F3-0413	J024148.3+424933.	$3.1 \pm 0.4$	5.45 (I06)	16.27	1.143	
M34-1-2476	9	J024148.7+424001.	$3.4 \pm 0.6$	4.83	15.82	1.11	
M34-4-2215	10	J024151.8+423822.	$1.7 \pm 0.5$	5.35	16.57	1.28	1.67
M34-4-2015		J024155.2+425031.	$1.4 \pm 0.3$	6.575 (I06)			2.04
	11	J024157.3+430026.	$4.9 \pm 0.8$	1.13	15.29	0.99	2.13
	12	J024159.5+424102.	$2.3 \pm 0.4$	4.19	12.98	0.67	
	J024201.7+424158.	$1.3 \pm 0.4$	1.978 (I06)				
M34-4-1524	13	J024205.8+424654.	$1.2 \pm 0.3$	8.27	14.34	0.99	1.35
	14	J024206.4+423621.	$3.1 \pm 0.6$	6.14	13.49	0.80	
	15	J024208.3+423843.	$2.8 \pm 0.6$	2.71	12.90	0.54	
	16	J024211.3+425035.	$2.6 \pm 0.4$	6.90	14.27	0.85	
	17	J024213.9+425547.	$2.8 \pm 0.5$	4.65	13.89	0.77	
M34-4-1436		J024217.2+424819.	$5.2 \pm 0.5$	1.179 (I06)			1.45
M34-1-1178	18	J024220.4+424905.	$0.6 \pm 0.2$	10.99	16.31	1.26	1.50
M34-4-1092	19	J024231.8+423711.	$8.0 \pm 1.3$	1.07	15.97	1.13	1.29
M34-1-1017		J024232.5+424907.	$14.1 \pm 0.8$	0.678 (I06)			2.35
M34-3-928		J024234.8+423926.	$1.1 \pm 0.4$	3.633 (I06)			1.09
M34-4-798	20	J024236.4+425433.	$9.2 \pm 1.1$	3.18	14.73	0.86	2.32
M34-4-631		J024241.9+424600.	$1.2 \pm 0.3$	7.322 (I06)			1.53
	21	J024242.5+424031.	$6.6 \pm 0.8$	1.97	12.62	0.52	
	22	J024243.6+425230.	$2.7 \pm 0.5$	10.75	15.59	1.18	
M34-3-523	23	J024247.5+424545.	$4.9 \pm 0.6$	1.19	16.45	1.20	1.04
	24	J024249.1+424013.	$4.5 \pm 0.7$	1.50	15.73	1.03	1.86
M34-4-316	25	J024250.8+425807.	$7.6 \pm 0.9$	0.94	14.51	0.84	
M34-3-279	26	J024251.7+424751.	$9.7 \pm 0.9$	3.67	12.78	0.64	1.37
M34-3-205		J024257.7+424147.	$5.2 \pm 0.8$	5.97 (I06)			
	27	J024258.2+425803.	$13.7 \pm 1.5$	1.55	14.78	0.86	
	28	J024259.5+424821.	$2.1 \pm 0.5$	10.52	15.49	1.25	1.18
		J024300.1+425801.	$13.5 \pm 1.5$	0.789 (I06)			
	29	J024301.9+424651.	$1.8 \pm 0.5$	0.49	17.67	1.44	
	30	J024320.9+424857.	$2.6 \pm 0.7$	8.85	15.74	1.18	0.84
	31	J024330.1+425307.	$8.9 \pm 1.5$	0.72	14.74	0.84	

**Notes.** The X-ray count rates (CR) in the 0.5–4.5 keV band have been extracted from the *XMM-Newton* Serendipitous Source Catalog using the energy conversion factor provided by Watson et al. (2009) for the pn camera equipped with a thick filter. The rotation periods are from M 11 or otherwise from I06 or J10 as indicated between brackets in the corresponding column. Extinction-corrected  $V_0$  magnitude and reddening-corrected  $(B - V)_0$  color indices are from M 11 and J10.  $V - I$  color indices are from I06.

**Table 2.** X-ray luminosity in the 0.5–4.5 keV band, X-ray to bolometric luminosity ratio, effective temperatures, mass, radius, rotation period, and Rossby number of M34 target stars.

Id.	2XMM identifier	$L_X$ ( $10^{28}$ erg s $^{-1}$ )	$L_{bol}$ ( $L_{\odot}$ )	$L_X/L_{bol}$ ( $10^{-3}$ )	$T_{eff}$ (K)	$M$ ( $M_{\odot}$ )	$R$ ( $R_{\odot}$ )	$P$ (d)	$Ro$	Seq.
1	J024126.0+424814.	13.9 ± 2.9	0.977	0.037 ± 0.008	5927	1.08	0.94	3.99	0.31	I
2	J024135.1+424103.	76.4 ± 6.2	0.395	0.500 ± 0.041	5303	(0.88)	0.74	0.90	0.05	C
3	J024136.6+425020.	72.3 ± 5.6	0.365	0.518 ± 0.040	5231	0.89	0.74	2.80	0.16	G
4	J024138.2+424403.	2.1 ± 1.5	0.578	0.010 ± 0.007	5470	(0.93)	0.85	5.99	0.37	I
5	J024138.5+423903.	15.0 ± 3.6	0.870	0.045 ± 0.011	5784	1.04	0.93	4.37	0.32	I
6	J024140.7+425446.	13.0 ± 3.1	1.225	0.028 ± 0.007	5964	1.09	1.04	2.80	0.22	I
7	J024143.9+424506.	13.9 ± 2.6	0.073	0.496 ± 0.094	4251	(0.63)	0.50	0.59	0.02	C
F4-0136	J024147.3+424339.	29.7 ± 3.5	1.044	0.074 ± 0.009	5855	1.05	0.99	2.87 (J10)	0.21	I
8	J024147.8+424121.	20.9 ± 3.7	3.006	0.018 ± 0.003	6078	1.25	1.56	6.06	0.59	I
F3-0413	J024148.3+424933.	22.5 ± 3.0	0.091	0.646 ± 0.085	4587	(0.70)	0.48	5.45 (I06)	0.23	G
9	J024148.7+424001.	24.2 ± 4.1	0.134	0.472 ± 0.081	4640	(0.71)	0.57	4.83	0.21	G
10	J024151.8+423822.	11.9 ± 3.6	0.082	0.379 ± 0.115	4349	(0.67)	0.50	5.35	0.21	G
M34-4-2215	J024155.2+425031.	10.1 ± 2.3	0.061	0.432 ± 0.097	3639	(0.66)	(0.62)	6.575 (I06)	0.26	G
11	J024157.3+430026.	35.1 ± 5.8	0.193	0.475 ± 0.078	4862	0.80	0.62	1.13	0.06	C
12	J024159.5+424102.	16.5 ± 3.1	1.264	0.034 ± 0.006	5653	1.11	1.17	4.19	0.34	I
M34-4-2015	J024201.7+424158	9.4 ± 2.8	0.035	0.705 ± 0.212	3558	(0.53)	(0.49)	1.978 (I06)	0.06	C
13	J024205.8+424654.	8.8 ± 2.1	0.462	0.050 ± 0.012	4862	0.87	0.96	8.27	0.47	I
14	J024206.4+423621.	22.2 ± 4.4	0.863	0.067 ± 0.013	5282	0.99	1.11	6.14	0.42	I
15	J024208.3+423843.	20.1 ± 4.0	1.271	0.041 ± 0.008	6117	1.14	1.00	2.71	0.23	I
16	J024211.3+425035.	18.6 ± 2.8	0.437	0.111 ± 0.016	5159	0.87	0.83	6.90	0.39	I
17	J024213.9+425547.	20.2 ± 3.4	0.584	0.090 ± 0.015	5359	0.92	0.89	4.65	0.28	I
M34-4-1524	J024217.2+424819.	37.2 ± 3.4	0.183	0.532 ± 0.048	4508	(0.75)	(0.70)	1.179 (I06)	0.05	C
18	J024220.4+424905.	4.5 ± 1.6	0.101	0.117 ± 0.042	4382	(0.68)	0.55	10.99	0.44	I
19	J024231.8+423711.	57.5 ± 9.0	0.119	1.263 ± 0.199	4605	(0.74)	0.54	1.07	0.05	C
M34-4-1092	J024232.5+424907.	101.0 ± 5.7	0.274	0.964 ± 0.054	4612	(0.86)	(0.82)	0.678 (I06)	0.04	C
M34-1-1017	J024234.8+423926	7.8 ± 2.9	0.024	0.845 ± 0.321	3380	(0.49)	(0.45)	3.633 (I06)	0.10	C
20	J024236.4+425433.	65.8 ± 7.7	0.288	0.597 ± 0.069	5136	(0.82)	0.68	3.18	0.17	G
M34-4-798	J024241.9+424600.	8.3 ± 2.3	0.029	0.746 ± 0.207	3403	(0.53)	(0.49)	7.322 (I06)	0.22	G
21	J024242.5+424031.	47.0 ± 5.5	1.631	0.075 ± 0.009	6198	1.16	1.11	1.97	0.17	I
22	J024243.6+425230.	19.5 ± 3.5	0.178	0.286 ± 0.051	4518	0.73	0.69	10.75	0.48	I
23	J024247.5+424545.	34.7 ± 4.2	0.083	1.093 ± 0.133	4483	(0.69)	0.48	1.19	0.05	C
24	J024249.1+424013.	32.2 ± 5.0	0.134	0.629 ± 0.097	4786	0.79	0.53	1.50	0.07	C
25	J024250.8+425807.	54.0 ± 6.7	0.348	0.405 ± 0.050	5183	(0.86)	0.73	0.94	0.05	C
26	J024251.7+424751.	69.4 ± 6.2	1.493	0.121 ± 0.011	5751	1.15	1.23	3.67	0.31	I
M34-4-316	J024257.7+424147.	36.9 ± 5.4	0.094	1.025 ± 0.150	3819	(0.75)	(0.70)	5.97 (I06)	0.27	G
27	J024258.2+425803.	98.1 ± 10.8	0.275	0.932 ± 0.103	5136	(0.84)	0.66	1.55	0.08	C
28	J024259.5+424821.	15.3 ± 3.3	0.212	0.189 ± 0.041	4399	0.74	0.79	10.52	0.47	I
M34-3-205	J024300.1+425801.	96.1 ± 11.0	0.182	1.380 ± 0.158	4474	(0.76)	(0.71)	0.789 (I06)	0.04	C
29	J024301.9+424651.	12.7 ± 3.5	0.038	0.875 ± 0.243	4086	0.62	0.39	0.49	0.02	C
30	J024320.9+424857.	18.5 ± 4.9	0.155	0.312 ± 0.083	4518	0.72	0.64	8.85	0.38	I
31	J024330.1+425307.	63.9 ± 11.1	0.281	0.594 ± 0.103	5183	0.88	0.66	0.72	0.04	C

**Notes.** The rotation periods are from M 11 or otherwise from I06 or J10, as indicated between brackets in the corresponding column. Mass and radius estimates between brackets are from I06. The last column gives the classification of each star as a member of the convective sequence (C), the interface sequence (I), or the gap (G).